SEDIMENTOLOGY the journal of the International Association of Sedimentologists IAS

Sedimentology (2025) **72**, 1233–1274 doi: 10.1111/sed.70000

Quantitative sedimentological analysis of the aeolian–fluvial Triassic Sherwood Sandstone Group, Cheshire Basin, UK

GRACE I. E. COSGROVE*, MAHMUD ALKATHERY*, MOHAMMED AL-MASRAHY*, LUCA COLOMBERA†, NIGEL P. MOUNTNEY* and DAVID B. THOMPSON*,[1]

**School of Earth and Environment, University of Leeds, Woodhouse, Leeds LS2 9JT, UK (E-mail: g.i.e.cosgrove@leeds.ac.uk)*

†Dipartimento di Scienze della Terra e dell'Ambiente, Università di Pavia, Via Ferrata 1, Pavia 27 100, Italy

Associate Editor – Charlie Bristow

ABSTRACT

Sedimentological analysis of the outcropping Sherwood Sandstone Group, northern Cheshire Basin, UK, documents the preserved stratigraphic expression of water table-controlled aeolian-dominated erg-margin successions (Wilmslow Sandstone Formation and lower Helsby Sandstone Formation), overlain by dryland fluvial deposits (middle Helsby Sandstone Formation). A quantitative assessment of sedimentary architectures and a comparison with analogous depositional systems reveals that strata of the Sherwood Sandstone Group are similar to other aeolian-dominated successions that also accumulated in rift basins, in erg-margin settings and where the water table interacted with the sediment surface. In stratal successions of erg-margin origin in the Wilmslow Sandstone Formation and Helsby Sandstone Formation, the dominant facies associations comprise: (i) thin cross-bedded dune sets characterized by foreset–toeset grainflow strata; and (ii) lenticular bodies of dry and damp-to-wet interdune strata. Together, these associations record accumulation of small, rapidly migrating transverse or oblique dunes, and intervening isolated interdune depressions. Two types of interdune deposits are observed: (i) near-horizontal wind-ripple laminated sandstone; and (ii) irregular to wavy-laminated sandstone with adhesion strata. These deposits indicate dry and damp–wet surface conditions, respectively. Dune climbing is demonstrated by the interfingering between dune toesets and interdune strata; this was enabled by accommodation generation driven by fault-related subsidence and associated relative water-table rise. Accumulation via climbing at very low angle but net positive, else by non-climbing mechanisms, is demonstrated by erosional, sharp dune–interdune bounding surfaces, which likely developed during slowdowns in subsidence rate. Episodic absolute water-table rise may have occurred during wet seasons or due to intense precipitation events, potentially in a monsoon climate. Water-table fluctuations may have also occurred in response to longer-term climatic perturbations following the Permian–Triassic mass extinction event. This study helps to constrain the factors controlling the accumulation of Triassic aeolian and mixed aeolian–fluvial successions, and their long-term preservation. Quantitative models are proposed to explain aeolian dune–interdune facies architectures. These can be used to guide predictions of three-dimensional sedimentary heterogeneity in the subsurface.

[1]Deceased.

Keywords Aeolian, erg, fluvial, margin, Permo-Triassic, quantitative, rift.

INTRODUCTION

Despite extensive global studies of outcropping successions of aeolian and partly aeolian origin, meaningful quantitative comparisons between successions whose accumulation was determined by different controlling factors remain difficult. Traditional aeolian facies models, developed from observations of both modern systems and ancient preserved successions, have sought to demonstrate and explain the stratigraphic complexities of these environments (e.g. Thompson, 1970a,b; Mckee *et al.*, 1971; Kocurek, 1981a,b; Loope, 1988; Langford, 1989; Mountney & Thompson, 2002; Mountney & Jagger, 2004; Mountney, 2006). However, these models are typically qualitative or, at best, semi-quantitative in form, and tend to be case-specific. Moreover, although significant advances have been made in understanding aeolian systems and controls acting thereon, making direct quantitative comparisons between individual case studies that document aeolian systems and their preserved sedimentary architectures remains challenging (Rodríguez-López *et al.*, 2014). To overcome this limitation and improve sedimentological and stratigraphic characterization, this study introduces a novel approach that integrates traditional outcrop-based data (including graphic logs, architectural panels and lithofacies descriptions) within a global relational database: the Database of Aeolian Sedimentary Architecture (DASA). This approach allows robust quantitative comparisons of an individual and specific outcrop case study – the Triassic Sherwood Sandstone of the UK Cheshire Basin – with a variety of globally distributed, aeolian systems, distributed under a variety palaeoenvironmental conditions.

Triassic aeolian and fluvial deposits present in many offshore and onshore sedimentary basins around the UK act as important hosts for geological resources (Bowman *et al.*, 1993; McKie *et al.*, 1998; Yaliz & Chapman, 2003; Fig. 1). The Lower Triassic Sherwood Sandstone Group (Fig. 2) has been the focus of considerable prior study due to its prominence as a fresh water aquifer (e.g. Holloway *et al.*, 1989), a geothermal energy source (e.g. Allen & Holloway, 1984; Downing *et al.*, 1984; Hirst *et al.*, 2015), a hydrocarbon reservoir (e.g. Burley, 1984; Bowman *et al.*, 1993; Meadows & Beach, 1993; Hogg *et al.*, 1996; Schmid *et al.*, 2004; Scorgie *et al.*, 2021), and as a potential repository for the temporary storage of hydrogen and the long-term disposal of carbon dioxide (e.g. Newell *et al.*, 2008; Armitage *et al.*, 2013, 2016; Payton *et al.*, 2021).

This study focusses on the Sherwood Sandstone Group of the Cheshire Basin, north-west England (Fig. 1). Numerous previous sedimentological investigations of the Sherwood Sandstone Group have attempted to document its preserved stratigraphic architecture within this rifted basin. Several studies have focussed on the Wilmslow Sandstone Formation and the Helsby Sandstone Formation to establish vertical and lateral lithofacies trends, and architectural-element distributions (e.g. Strahan, 1882; Maidwell, 1911, 1914, 1915; Thompson, 1969, 1970a,b; Øxnevad, 1991; Benton *et al.*, 1994; Mountney & Thompson, 2002; Meadows, 2006). Although sedimentological data have been collected previously, numerous well-exposed outcropping successions have remained undocumented in detail. This study compiles and integrates new and available legacy data to develop a comprehensive series of quantitative facies models for this succession. In this context, the focus is on the outcrops within the northern Cheshire Basin and its transitional region to the adjoining East Irish Sea Basin.

In part, the Wilmslow Sandstone Formation and Helsby Sandstone Formation of the Sherwood Sandstone Group record examples of ancient water-table influenced aeolian systems, in which aeolian dune and damp-to-wet and dry interdune deposits interfinger laterally and alternate vertically. These aeolian deposits occur locally interbedded with dryland fluvial deposits (Thompson, 1970a,b; Mountney & Thompson, 2002). Although examples of wet aeolian systems and their preserved successions are now extensively documented in the literature (e.g. Kocurek, 1981a,b; Pulvertaft, 1985; Glennie, 1990; Meadows & Beach, 1993; Herries & Cowan, 1997; Gross *et al.*, 2023), many such studies are largely qualitative in nature and do not quantify variability in the lithology,

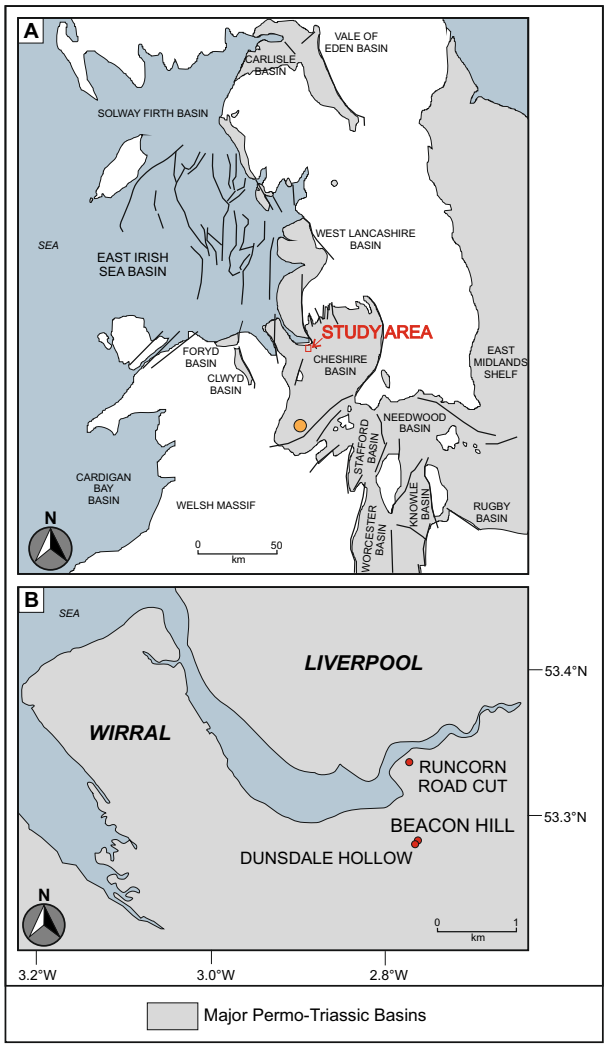

Fig. 1. (A) Map of the Central and North West England showing the distribution of major Permo-Triassic basins (after Coward, 1995). The orange circle indicates the location of the Prees Borehole. The study area is highlighted in a red box and shown in detail in part B. (B) Red circles indicate the location of study sites detailed in this investigation: Runcorn Road Cut, Beacon Hill and Dunsdale Hollow.

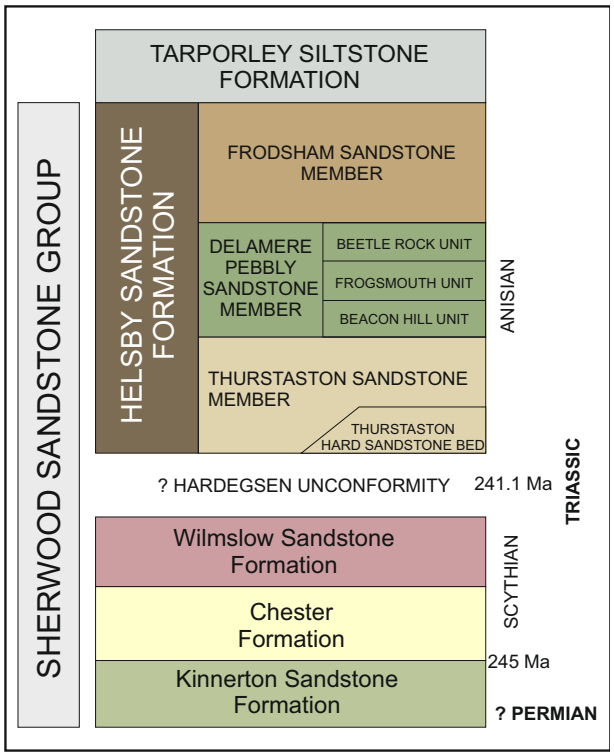

Fig. 2. Stratigraphic subdivisions of the Sherwood Sandstone Group in the Cheshire Basin (after Harland *et al.*, 1990; Mountney & Thompson, 2002).

thickness, lateral extent and continuity of architectural elements in these successions. Given the broad applied significance of the Sherwood Sandstone Group – notably in relation to carbon capture and underground storage, geothermal energy generation, hydrogen storage and groundwater use – quantifying the architectural complexities of these successions is especially important because the sedimentology of the deposits exerts a fundamental control on fluid-flow behaviour in these lithologically heterogeneous successions.

The aim of this study is to document the architectural complexity of a mixed wet–dry aeolian erg-margin succession, to explain controls on the evolution of the formative sedimentary systems, and to quantitatively compare the deposits of the Sherwood Sandstone Group with other analogous aeolian-dominated systems. Specific research objectives are as follows. (i) To demonstrate the sedimentological variability seen in the Wilmslow Sandstone Formation and Helsby Sandstone Formation in the northern Cheshire Basin with new outcrop data. (ii) To undertake a comprehensive quantification of the geometry, spatial relationships and lithological heterogeneity of aeolian and fluvial architectural elements of the Wilmslow Sandstone Formation and Helsby Sandstone Formation in the northern Cheshire Basin. (iii) To quantitatively compare the sedimentological architecture of the Wilmslow Sandstone Formation and Helsby Sandstone Formation with analogous ancient aeolian successions. Fluvial deposits are

considered here only where they occur in close association with aeolian deposits: a comprehensive discussion of the sedimentology of fluvial deposits of the Sherwood Sandstone Group is beyond the scope of this study.

BACKGROUND: WATER-TABLE INFLUENCED WET AEOLIAN SYSTEMS

Both modern aeolian systems and their preserved successions are commonly classified as dry, wet or stabilizing (Kocurek & Havholm, 1993). The Helsby Sandstone Formation is an example of a mixed wet and dry aeolian system that varied between these states both spatially and temporally (Mountney & Thompson, 2002). Wet aeolian systems develop where accumulation is regulated by the progressive rise of the water table, which occurs coincidently with aeolian activity – notably dune migration (Fig. 3; Kocurek *et al.*, 1992; Crabaugh & Kocurek, 1993). Preserved interdune units associated with aeolian dune units record the influence of the water table on aeolian system construction, accumulation and preservation (Kocurek *et al.*, 1992; Crabaugh & Kocurek, 1993). Accumulated wet-interdune architectural elements tend to remain constant in thickness when, through times of formative interdune translation in front of advancing dunes, the rate of the water-table rise remains in balance with the rate of aeolian dune and interdune migration (Mountney, 2012). If either one of these variables changes, dunes will expand into interdune areas (eventually creating a dry system), else will contract allowing expansion of the interdune flats (Crabaugh & Kocurek, 1993; Kocurek & Havholm, 1993). Wet aeolian systems may also be flooded by high-intensity, flash-flood rainfall events, particularly in erg margins (Langford, 1989; Herries, 1993). Where interdune corridors are open to dune-field margins, they may be subject to fluvial incursions (Langford, 1989). Where interdunes form enclosed depressions, rainfall may run-off from adjacent dunes to form temporary interdune ponds (Mountney, 2006).

Wet interdunes are composed of deposits that accumulate on substrates submerged by the water table or flood waters, to the extent that the interdunes are continuously or intermittently flooded (Kocurek & Havholm, 1993; Loope *et al.*, 1995; García-Hidalgo *et al.*, 2002). Wet interdunes are characterized by a diverse range of sedimentary structures, such as for example subaqueous current and wave ripples, wavy laminations, contorted bedding (all deposited under wet conditions), adhesion structures, bioturbation structures and desiccation cracks (all deposited under damp conditions) (Ahlbrandt & Fryberger, 1981; Hunter, 1981; Kocurek, 1981a). Where the fringes of wet interdunes dry out, wind-ripple lamination may be present (Mountney, 2006).

In wet aeolian systems, the stratigraphy may exhibit two distinct styles, in relation to climbing (e.g. Crabaugh & Kocurek, 1993; Kocurek & Havholm, 1993; Carr-Crabaugh & Kocurek, 1998) and non-climbing accumulation (e.g. Simpson & Loope, 1985; Loope & Simpson, 1992; Fig. 3).

Accumulation models

In wet aeolian systems, migrating dunes can accumulate – and their deposits may become preserved – in response to a gradual rise in the level of the water table (Crabaugh & Kocurek, 1993; Kocurek & Havholm, 1993; Carr-Crabaugh & Kocurek, 1998). The angle of climb of dune sets and associated wet interdune elements is governed by the ratio between the rate of water-table rise and the rate of bedform migration. Models presented by Rubin (1987) and Kocurek & Havholm (1993) propose that increasing dune-set thicknesses and bedform migration angles should be associated with concomitant increases in the thicknesses of interbedded interdune elements, for dunes and interdunes of fixed size (Fig. 3; Hunter, 1977a; Rubin, 1987; Kocurek & Havholm, 1993). The expansion and contraction of interdune flats between dune forms are determined by the availability of sediment suitable for aeolian dune construction and affect the geometry of preserved dune and interdune strata. (Crabaugh & Kocurek, 1993; Kocurek & Havholm, 1993; Mountney, 2012). A greater external sediment supply is required to maintain dune migration and climbing for faster rates of relative water-table rise (Mountney, 2012). In response to changes in sediment availability for dune construction, the size and extent of dunes and adjoining wet or damp interdunes varies. An increase in the rate of water-table rise tends to restrict the supply and availability of sediment for aeolian construction, thereby favouring a decrease in dune size and an associated increase in the size of wet interdune flats (Kocurek & Havholm, 1993; Kocurek, 1999; Mountney & Thompson, 2002; Mountney & Jagger, 2004; Mountney, 2012).

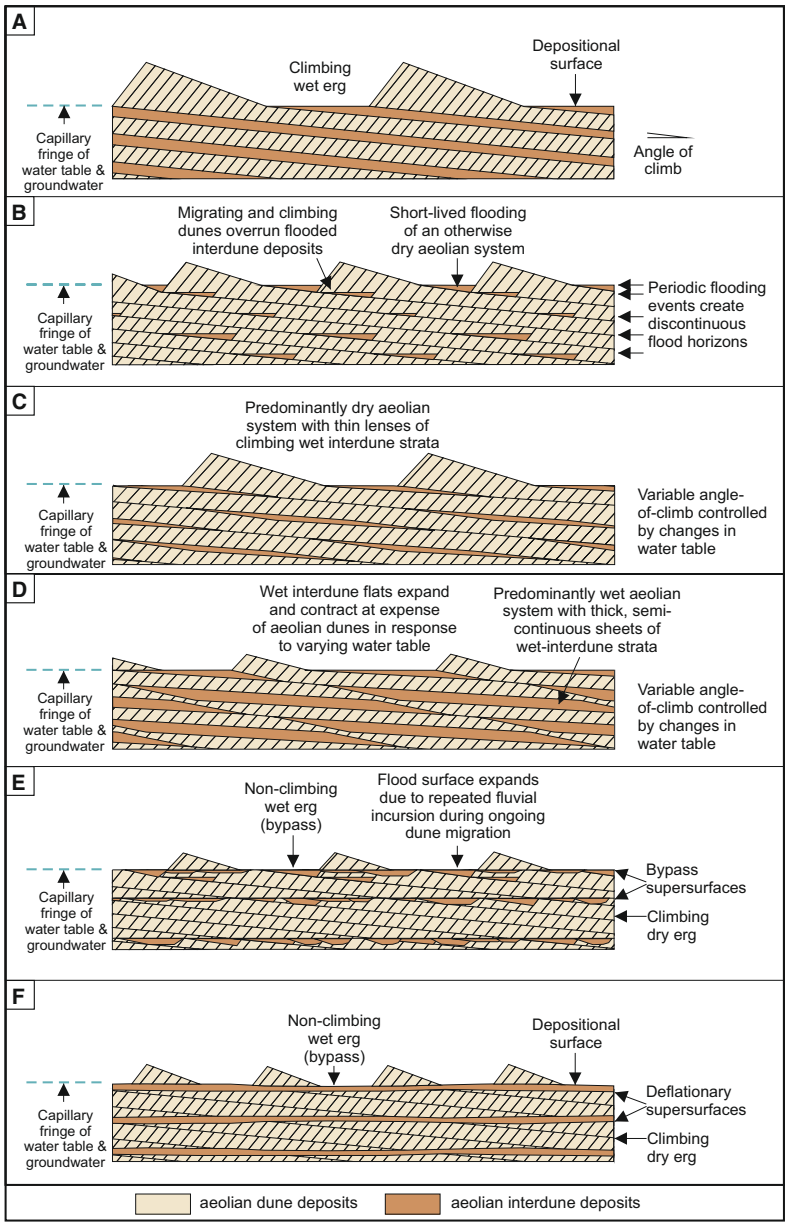

Fig. 3. Different types of interdune-element geometries determined by changes in rates of: (i) water-table rise; (ii) the rate of aeolian-dune migration; and (iii) the net aeolian sediment budget. (A) Entrada Sandstone, Utah, USA (Kocurek, 1981a); (B) Navajo Sandstone, Utah, USA (Herries, 1993); (C, D) Helsby Sandstone Formation, Cheshire, UK (Mountney & Thompson, 2002); (E) Cedar Mesa Sandstone, Utah USA (Langford & Chan, 1988; Langford, 1989); (F) White Sands, New Mexico, USA (Simpson & Loope, 1985; Loope & Simpson, 1992). Parts (A) and (F) show contrasting end-member models for the accumulation of wet interdune strata. In Part (A), wet aeolian system with dunes and interdunes climb under the influence of a progressively rising water table. In Part (F), non-climbing dunes migrating across extensive interdune flats. After Crabaugh & Kocurek (1993) and Mountney & Thompson (2002).

A temporally persistent state of sediment bypass leads to a zero angle of bedform climb, resulting in no or negligible aeolian-sediment preservation (e.g. McKee & Moiola, 1975; Simpson & Loope, 1985; Loope & Simpson, 1992; Kocurek & Havholm, 1993). In cases where the angle of climb is positive overall but fluctuates around positive and negative values, else, where it is zero over shorter timescales, the accumulation and ultimate preservation of interdune elements in the stratigraphic record can be more complicated (Kocurek *et al.*, 1992; Kocurek & Havholm, 1993; Basilici *et al.*, 2021). In these systems, dune sets will only accumulate as limited preservation space becomes available in relation to slow and potentially punctuated episodes of water-table rise (Fig. 3; McKee & Moiola, 1975; Simpson & Loope, 1985; Loope & Simpson, 1992; Kocurek & Havholm, 1993). As such, significant episodes of sediment bypass are likely to occur. In this way, the depositional record may record amalgamated wet-interdune elements, possibly incorporating thin aeolian dune toeset deposits. The dominantly wet-interdune deposits are bounded by one or numerous unconformities (Simpson & Loope,

1985; Loope & Simpson, 1992; Kocurek & Havholm, 1993). However, such surfaces are difficult to identify since they are diastems (paraconformities) that separate thin (typically millimetre to decimetre) bundles of similar strata that become vertically stacked over long time periods.

GEOLOGICAL SETTING

The Cheshire Basin is one of a series of linked rift basins of north-west Europe that formed during the early stages of the break-up of the Pangean supercontinent, associated with an early phase of Atlantic opening (Griffiths *et al.*, 2003; Ziegler & Dèzes, 2006). In north-west England, Triassic basins form a major north–south trending rift system that extends for >400 km from the Solway Firth and Carlisle basins in the north, through the Vale of Eden, Cumbria, Lancashire, East Irish Sea, Cheshire, Stafford, Needwood, Shropshire and Worcester–Knowle Basins in the English midlands (Chadwick, 1997), and further south to the Wessex Basin. The Cheshire basin itself forms a half-graben, bounded to the east by the Wem–Red Rock fault system (Chadwick & Evans, 1995; Chadwick, 1997); at its western margin, Permo-Triassic strata onlap onto older Carboniferous limestones and pre-Carboniferous crystalline basement rocks (Colter & Barr, 1975; Evans, 1990; Ruffell, 1995; Chadwick, 1997).

During the Early to Mid-Triassic, north-west England was situated *ca* 15° north of the palaeo-equator in the northern part of the Pangean supercontinent, Laurasia (Warrington & Ivimey-Cook, 1992; Benton *et al.*, 1994). The latitudinal position of the Cheshire Basin during this period was comparable to that of the modern-day Sahara (Glennie, 1983). At the time of deposition, the prevailing climatic conditions were arid to semi-arid (Thompson, 1970a,b). The fill of the Cheshire Basin is composed of a series of major units, deposited between 260 to 230 Ma, which collectively make-up the Sherwood Sandstone Group. From oldest to youngest, these are: (i) the Kinnerton Sandstone Formation (Induan to Olenekian age 251.9 to 247.2 Ma); (ii) the Chester Formation or "Pebble Beds" (Olenekian age; 251.2 to 247.2 Ma); (iii) the Wilmslow Sandstone Formation (Olenekian age; 251.2 to 247.2 Ma); (iv) the Helsby Sandstone Formation (Anisian age; 247.2 to 242 Ma). The Mercia Mudstone Group (MMG; Anisian – Rhaetian age; 247.2 to 201.4 Ma) overlies the Sherwood Sandstone Group (Warrington *et al.*, 1980; Warrington & Ivimey-Cook, 1992). The Triassic Penarth Group is also present in the Cheshire Basin, but is not found in the study area (Warrington *et al.*, 1980; Waters & Lawrence, 1987). Based on seismic, core and well-log data, the Sherwood Sandstone Group and Mercia Mudstone Group, and overlying Jurassic sediments within the Cheshire Basin depocentre have a total thickness of *ca* 4000 m (Chadwick, 1997). However, the Sherwood Sandstone Group and Mercia Mudstone Group thin markedly to *ca* < 300 m at a position within 10 km of the northern margin of the basin between Runcorn and the Wirral (Plant *et al.*, 1999).

In northern Cheshire, the Sherwood Sandstone Group is predominantly composed of sandstone and conglomerate with minor siltstone and mudstone units of continental origin. Units of these lithologies mainly accumulated in a variety of mixed fluvial and aeolian environmental settings (Thompson, 1969, 1970a,b; Warrington *et al.*, 1980). The deposits of the Sherwood Sandstone Group broadly comprise the following facies associations: (i) conglomeratic and sandstone fluvial channel deposits with subordinate interbedded siltstone and mudstone fluvial overbank deposits; and (ii) aeolian dune-set sandstone with interbedded sandstone, siltstone and mudstone interdune deposits. Regionally, the Sherwood Sandstone Group forms the dominant fill of the genetically related and partially interlinked onshore rift basins, and the offshore East Irish Sea Basin (Thompson, 1970a,b; Chadwick & Evans, 1995; Meadows, 2006).

In the Sherwood Sandstone Group of the northern Cheshire Basin, the Helsby Sandstone Formation, previously known as the Keuper Sandstone, unconformably overlies the Wilmslow Sandstone Formation, previously known as the Upper Mottled Sandstone (Warrington *et al.*, 1980; Evans *et al.*, 1993). The Wilmslow Sandstone Formation comprises red-brown to brick-red, fine to medium-grained cross-bedded sandstones, which are occasionally intercalated with siltstones. The overlying Helsby Sandstone Formation comprises fine to medium-grained, occasionally micaceous, cross-bedded and flat-bedded sandstones. Pebbly sandstone and conglomerate beds with clasts of both extraformational and intraformational origin are prevalent in the basal 20 m of the Helsby Sandstone Formation, and also occur intermittently in the middle part of the Helsby Sandstone Formation.

Additionally, thin (<0.5 m) lenticular beds of reddish-brown siltstone and mudstone are present, commonly occurring in sequences that fine upward. Calcretes and rhizoliths are observed locally in the south-west and central parts of the Cheshire Basin (Purvis & Wright, 1991; Mountney & Thompson, 2002; Hounslow & McIntosh, 2003; Newell, 2006). Both the Wilmslow Sandstone Formation and Helsby Sandstone Formation have long been interpreted to be of mixed aeolian–fluvial origin (e.g. Thompson, 1970a,b).

The Helsby Sandstone Formation is the thickest unit in the Cheshire Basin, and attains a maximum recorded thickness of *ca* 230 m in the Prees borehole (Fig. 1; Evans *et al.*, 1993). In the northern part of the Cheshire Basin, in the area around the towns of Helsby, Frodsham and Runcorn, and north-westwards to the Wirral, the Helsby Sandstone Formation is further subdivided into three members: (i) the basal Thurstaston Soft Sandstone Member (dominantly aeolian with minor fluvial deposits); (ii) the middle Delamere Pebbly Sandstone (dominantly fluvial deposits); and (iii) the upper Frodsham Soft Sandstone Member (dominantly aeolian deposits) (Thompson, 1970b; Warrington *et al.*, 1980; Mountney & Thompson, 2002). The Helsby Sandstone Formation and its members crop out extensively in the north-west part of the Cheshire Basin. However, establishing lateral stratigraphic correlations across the region is challenging due to the presence of multiple faults and lateral stratigraphic variability.

METHODS

Outcrop analysis

Outcrop data have been collected from a series of natural outcrops and roadcuts in and around the towns of Frodsham, Runcorn and Helsby, north-west England (Fig. 1). Specific outcrops considered here include those at Beacon Hill, Dunsdale Hollow and Runcorn Expressway road cutting (Fig. 1). Data have been compiled into a series of two-dimensional panels (Figs 9 to 11), which portray sedimentological information identified in a single, approximately planar outcrop face. Panels depict successions that vary in thickness between 8 m and 16 m and in length between 50 m and 209 m. Panels have been generated from detailed field drawings, measurements and photomosaics. New data presented here record: (i) the lateral and vertical extent of architectural elements; (ii) the distinctive sedimentary structures and stratification types present in architectural elements; (iii) the spatial arrangement of architectural elements; and (iv) the nature of the surfaces that bound them. Panels have been assembled to form composite fence diagrams – which record outcrops for which there is continuity of exposure – to create, where possible, a pseudo-three-dimensional representation of the stratigraphic architecture. This allows architectural elements to be traced in three-dimensions. These data are used to infer palaeo-flow and palaeo-transport direction (see Rubin & Hunter, 1983); panels have been constructed oriented parallel, perpendicular and oblique to the reconstructed primary direction of aeolian bedform migration (south-west; Fig. 12), depending on the orientation of outcropping cliff faces. The panels are supplemented by three representative vertical graphic logs (cumulative length 30 m; Fig. 12). Over 400 readings of palaeocurrent data (comprising foreset dip magnitude and azimuth data from cross-bedded sets) were collected from both aeolian (264 palaeocurrent readings) and fluvial (150 palaeocurrent readings) facies units. Summaries of these data are presented as rose diagrams for each section (Fig. 12).

Lithofacies are here defined as sedimentary bodies differentiated on the basis of sediment composition, structure, texture, fossil content, bedding geometry and nature of their bounding surfaces (Walker, 1984; Reading, 1986). The lithofacies are grouped according to the architectural element in which they are found, which are themselves classified as aeolian dune elements, aeolian interdune elements, channelized fluvial elements and non-channelized fluvial elements. Herein, architectural elements are described and interpreted in detail. They are defined as distinct sedimentary bodies with characteristic architectural features (size, shape, geometry, internal facies organization) and that are the product of deposition in a specific sub-environment.

Although tectonic tilting is a recognized geological process that can affect sedimentation and basin development, it was not explicitly accounted for in this study. Palaeohorizontal surfaces were determined from the attitude of interdune elements, which are themselves interpreted to represent a palaeo-accumulation surface – that is, an imaginary surface that connects

multiple neighbouring interdune hollows that would have originally been coevally developed (sensu Kocurek *et al.*, 1992; Mountney & Howell, 2000; Mountney, 2006).

Quantitative analysis

Quantitative analysis of the architecture of the Sherwood Sandstone Group has been completed using the Database of Aeolian Sedimentary Architecture (DASA; Cosgrove *et al.*, 2021a), which stores data on aeolian and interdigitated non-aeolian geological bodies. Quantitative data from the Sherwood Sandstone Group (described in detail below) have been collated from the original outcrop study presented herein.

The Sherwood Sandstone Group has been compared with 87 other ancient aeolian successions, each of which is classed as a case study. A full list of all the case studies and source literature used in this investigation are included in the Supplemental Material (Table S1). All case studies are associated with ancillary data on its geological background, which were collated from the wider literature. Ancillary data include: geological age, tectonic (basin) setting, climatic conditions (icehouse or greenhouse) and dune-field physiographic setting (i.e. central versus marginal erg setting). Primary data were extracted from published material, including outcrop panels, sedimentary logs and core logs. For all architectural elements, the thickness and length measurements represent the maximum observable (or recorded) thickness or length of an architectural element, as presented in an outcrop panel, for example. Lengths are recorded parallel to the overall inferred or reported direction of bedform migration. The proportions of architectural elements in successions, or in parts thereof, are presented as fractions of the total recorded thickness.

Following similar methods to those employed in Cosgrove *et al.* (2021a, 2022), data on element thicknesses have been analysed statistically. Two-tailed t-tests have been undertaken to determine if a significant difference exists between mean values across Precambrian and Phanerozoic groups. The statistical significance of differences across groups are expressed as a *P*-value (P). In all statistical analyses, the *P*-value has been considered significant for $\alpha < 0.05$, to determine if the null hypothesis is rejected. For all bivariate analyses, the coefficient of determination (R^2) of power laws has been determined.

RESULTS

Results are separated into: (i) analysis of sedimentary facies; and (ii) quantitative analysis and comparison of the Sherwood Sandstone Group with comparable sedimentary systems.

Sedimentary facies

Fifteen aeolian and fluvial lithofacies are recognized (Table 1; Figs 4 to 8). Summary descriptions of all lithofacies are included in Table 1. Lithofacies are interpreted below and grouped according to the type of architectural element (e.g. fluvial channel, aeolian dune) in which they are found. In this regard, groups of genetically related facies encountered within the architectural elements form facies associations. The main architectural-element types with which these lithofacies are associated are described below.

Aeolian dune facies

Five facies are associated with aeolian dune architectural elements.

Aeolian dune facies 1: Mixed Grainflow and wind-ripple strata

Observations. Aeolian Dune Facies 1 comprises packages of high-angle dipping (>15°), inversely graded, cross-strata, inclined at angles up to 23°. These packages pinch-out downslope (Fig. 4A). Grains commonly have a 'millet-seed' texture (Fig. 4B). These packages are separated by translatent and climbing strata that lack internal ripple-form lamination. The interbedding of these stratal packages results in a bimodal grain-size distribution.

Interpretation. Aeolian Dune Facies 1 accumulated by successive avalanches of sand down dune slipfaces (Hunter, 1977a,b, 1981). The dune slipface underwent gravitational collapse, leading to the accumulation of Aeolian Dune Facies 1. The inverse grading associated with Aeolian Dune Facies 1 arose from kinetic sieving during avalanche movement down the dune slipface (Loope *et al.*, 2012). These stratal packages and the associated translatent strata are grainflow and wind-ripple deposits, respectively. Aeolian dunes are most commonly composed of mixed grainflow and wind-ripple strata (Fig. 4A).

Table 1. Summary information outlining the aeolian facies associations in the Sherwood Sandstone Group.

Aeolian Lithofacies							
Facies	Colour	Grain-Size	Thickness	Texture	Facies Characteristics	Occurrence	Architectural Element
AD1: Moderate to high-angle grainflow strata	Reddish-brown and orange	Fine to coarse-grained sand	Set thickness = 0.1 –1.0 m; foreset thickness = 10 –60 mm	Well to very well-sorted; rounded grains	Aeolian dune high-angle cross-strata (up to 23°); aeolian dune foresets are grainflow dominated; grainflow strata pinch-out towards the base of the lee slope; grains have a millet-seed texture; dune strata are truncated in places by erosional surfaces; alternating grainflow deposits are separated by thin wind-ripple laminae leading to bimodal grain-size distributions and pinstripe lamination	Dune leeside foresets (very common)	Aeolian Dune
AD2: Moderate-angle grainfall strata	Reddish-brown and brown	Fine to medium-grained sand	Set thickness = 0.1 –0.3 m; foreset thickness = 1 –3 mm	Well to very well-sorted; rounded grains	Small-scale dune cross-strata; alternating grainflow and grainfall strata (bimodal grain-size); concordant cyclic cross-beds; reactivation surfaces are present	Dune leeside foresets (rare)	Aeolian Dune
AD3: Low-moderate angle wind-ripple strata	Orange and brown	Medium to very coarse-grained	Set thickness = 0.1 –0.6 m; laminae rarely exceed 10 mm	Moderately to well-sorted; sub-rounded to rounded grains	Low-angle cross-strata in an aeolian dune (up to 12°) formed from packages of translatent wind-ripple strata; bimodal grain-size distribution associated with pinstripe lamination; laminae pinch out laterally and interfinger with interdune facies	Dune leeside toesets (common)	Aeolian Dune
AD4: Massive Sandstone	Reddish brown and orange	Medium to coarse-grained	Set thickness = 0.15 –2.0 m	Well to very well-sorted; rounded to well-rounded grains	Homogeneous sediment texture with frosted grains; in some places very faint (vague) aeolian dune high-angle cross-lamination (up to 22°) is present; rhizoliths, iron oxide concretions and calcite cements are present	Dune foresets (common)	Aeolian Dune

Table 1. (continued)

Aeolian Lithofacies							
Facies	Colour	Grain-Size	Thickness	Texture	Facies Characteristics	Occurrence	Architectural Element
AD5: Soft-sediment deformed sandstone	Reddish brown and orange	Fine to coarse-grained sand	Set thickness = 0.1 –1.0 m; foreset thickness = 10 –50 mm	Moderately to well-sorted; rounded grains	Dune cross-stratified strata (intercalated packages of grainflow and wind-ripple strata) showing soft-sediment deformation in dune toesets that overlie or interdigitate with damp interdune strata	Dune plinth or apron (rare)	Aeolian Dune
ID1: Horizontal to sub-horizontal laminated sandstone	Reddish brown and brown	Fine to very coarse-grained sand	Set thickness = 0.1 –1.0 m	Moderately to well-sorted; subrounded grains	Sub-horizontal, discontinuous translatent wind-ripple strata	Areas with depressed water table (common)	Aeolian Interdune
ID2: Wavy laminated sandstone	Reddish brown, orange and white-grey	Fine to very coarse-grained sand	Set thickness = 0.1 –1.0 m	Moderately to well-sorted; subrounded grains	Wavy to crinkly laminated sandstone; adhesion ripples and small-scale flame structures are present; downfolded laminations in set tops are sometimes present	Areas with elevated water table (very common)	Aeolian Interdune

Aeolian dune facies 2: Grainfall strata

Observations. Aeolian Dune Facies 2 consists of moderate-angle dipping (up to 18°), thin, parallel-cross-laminated strata, which have a uniform thickness (Fig. 4C and D). Sandstone deposits of Aeolian Dune Facies 2 are very-well sorted and composed of very fine to fine grains. Deposits of Aeolian Dune Facies 2 occur draped over grainflow strata (Aeolian Dune Facies 1; Hunter, 1977a,b) and thus occur locally interbedded with Aeolian Dune Facies 1 (mixed grainflow and wind-ripple strata).

Interpretations. Aeolian Dune Facies 2 are deposits that form when the wind transports clouds of saltating grains beyond the dune brink; reduced wind velocity in lee-side depressions causes transport capacities to reduce and grains to settle out onto the lee slopes (Nickling *et al.*, 2002). Aeolian Dune Facies 2 are grainfall strata.

Aeolian dune facies 3: Wind-ripple strata

Observations. Aeolian Dune Facies 3 comprises low to moderate-angle, asymmetrical, cross-stratified, translatent and climbing strata (Fig. 4E and F). These strata lack internal ripple-form lamination. Commonly, Aeolian Dune Facies 3 displays inverse grading of laminae. Changes in colour conferring a pinstripe appearance to the lamination highlight this inverse grading (Fryberger & Schenk, 1988). Aeolian Dune Facies 1 (mixed grainflow and wind-ripple strata) commonly overlies and merges downdip with Aeolian Dune Facies 3.

Interpretation. Aeolian Dune Facies 3 forms when wind-blown saltating grains strike other sand grains obliquely. During this process, they propel other grains forward (Bagnold, 1941; Hunter, 1977a,b). Aeolian Dune Facies 3 accumulates through the migration of aeolian ripples either down or across the lower part of the dune slipface. Aeolian Dune Facies 3 are wind-ripple strata (Hunter, 1977a,b, 1981).

Aeolian dune facies 4: Homogenous sandstone with rhizoliths

Observations. Aeolian Dune Facies 4 generally comprises homogenous sandstones that are internally massive and lack any clear stratification. Locally, very faint (vague) high-angle cross-lamination (up to 22°) is present (Fig. 4G). Aeolian Dune Facies 4 contains elongate mineralized, hardened nodules with irregular edges. Nodule dimensions are typically *ca* 50 mm × 400 mm (Fig. 4G). Aeolian Dune Facies 4 is commonly found in the foresets of aeolian dunes.

Interpretations. Aeolian Dune Facies 4 are homogenous sandstones with rhizoliths. Aeolian Dune Facies 4 may have accumulated by the fall-out of sand from suspension under sustained reductions in wind velocity. The sustained fall-out of sand would have been necessary for a prolonged time period to accumulate the observed sets of massive sand. Alternatively, the apparently massive nature of Aeolian Dune Facies 4 may have originated from grainflow or wind-ripple processes, where grain-size segregation and differentiation do not occur, resulting in uniformity in grain size. In such cases, observable stratification planes may not always be present (e.g. Campos-Soto *et al.*, 2022). The hardened nodules in Aeolian Dune Facies 4 are interpreted as rhizoliths, taking the form of calcite concretions around relic plant-root structures (cf. Mount & Cohen, 1984; Jones & Ng, 1988; Loope, 1988). These rhizoliths indicate the stabilization of dunes by vegetation (Mountney, 2006).

Aeolian dune facies 5: Convoluted Grainflow and wind-ripple strata

Observations. Aeolian Dune Facies 5 comprises intercalated packages of grainflow (Aeolian Dune Facies 1) and wind-ripple strata (Aeolian Dune Facies 3) that are convoluted (Fig. 4H and I), typically displaying intra-dune folding (Fig. 4H and I). It is locally present in the lower part of dune foresets and in dune toesets. Aeolian Dune Facies 5 occurs in close association with Interdune Facies 2 (wavy laminated interdune strata; see below).

Interpretations. Aeolian Dune Facies 5 is interpreted to be formed via post-depositional soft-sediment deformation. Intra-dune folding indicates near-surface liquefaction of the slumping of moderately cohesive, moist sands on the dune lee-slope in response to sediment surface wetting (Doe & Dott Jr., 1980). In places, larger-scale deformation structures within Aeolian Dune Facies 5 may indicate liquefaction below the water table (McKee *et al.*, 1971); this can occur via the loading of saturated sand by the advance of overriding dunes (Horowitz, 1982; Collinson, 1994).

Aeolian interdune facies

Interdune Facies 1 and Interdune Facies 2 (Fig. 5) are associated with aeolian interdune elements.

Interdune facies 1: Dry interdune strata

Observations. Interdune Facies 1 comprises horizontal to sub-horizontal, translatent sandstone laminae that lack internal rippleform lamination (Hunter, 1977a,b, 1981). Facies ID1 is typically gradationally overlain by Aeolian Dune Facies 3 (wind-ripple strata) and can interfinger laterally with facies Interdune Facies 2 (Fig. 5).

Interpretations. Interdune Facies 1 are interpreted to be wind-ripple strata that accumulated via the migration of aeolian ripples across a dry interdune surface. Facies Interdune Facies 1

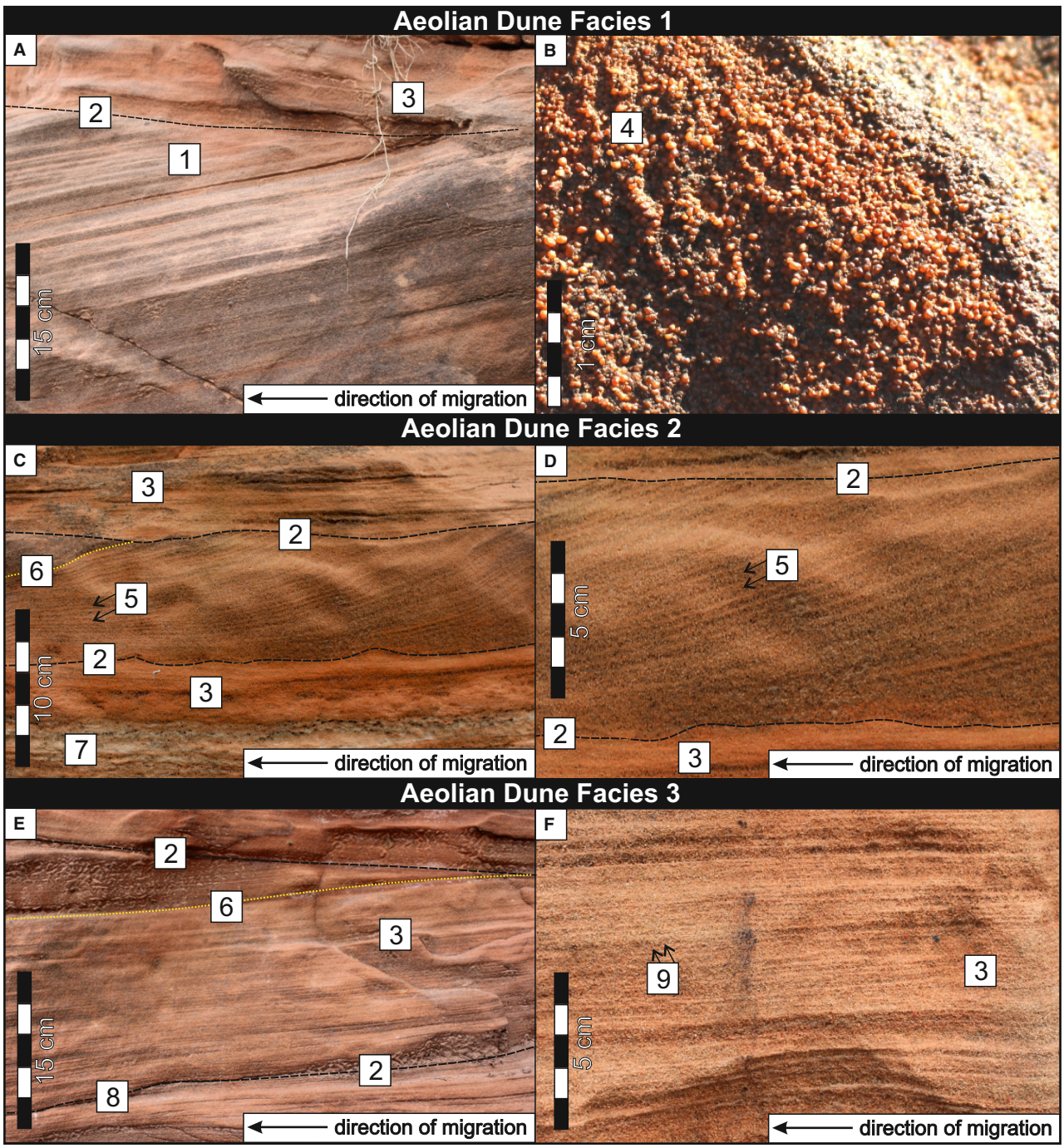

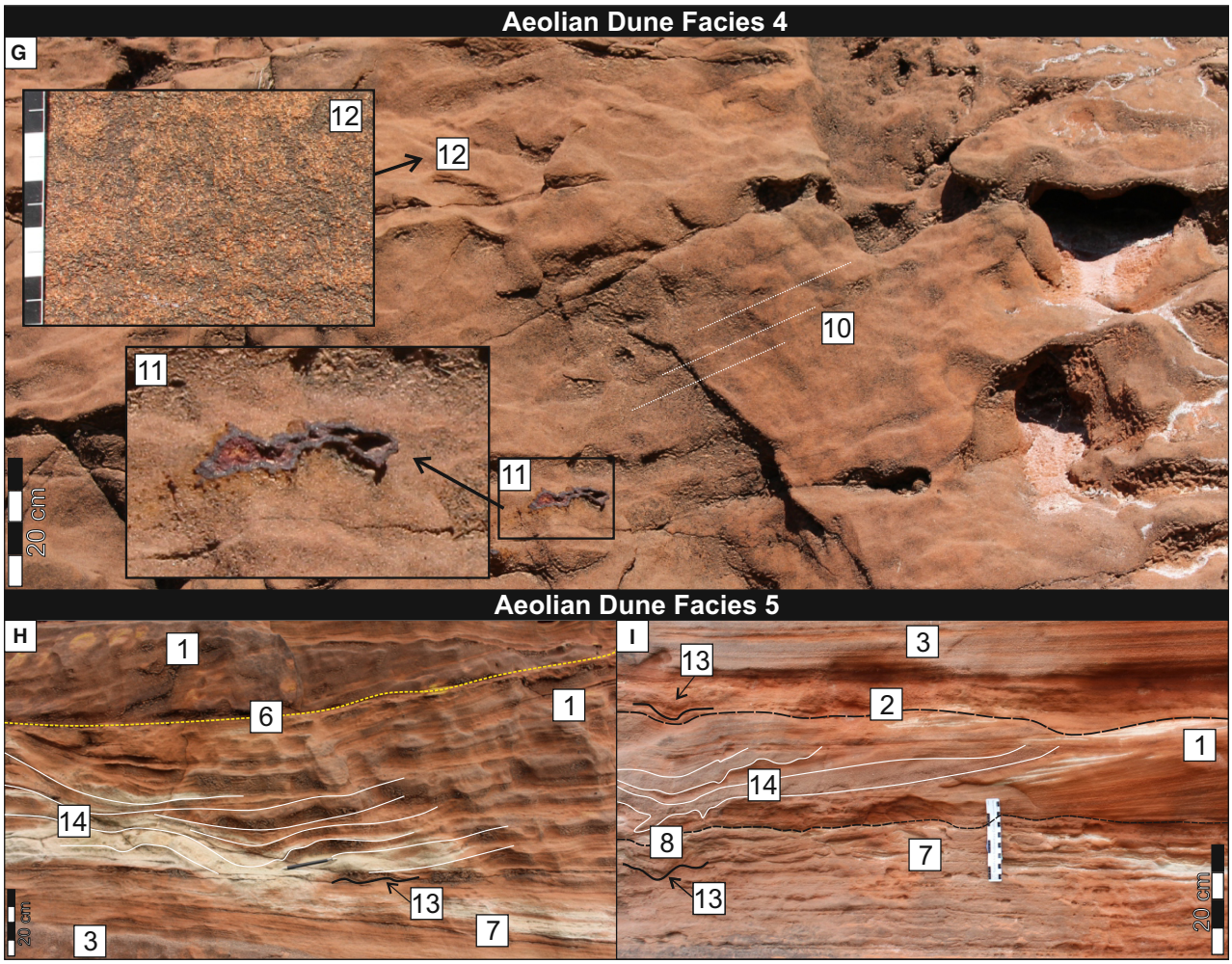

Fig. 4. Examples of aeolian dune facies; in all images numbers denote points of interest, described below. (A) and (B) Aeolian Dune Facies 1 (moderate to high angle grainflow strata); (C) and (D) Aeolian Dune Facies 2 (moderate angle grainfall strata); (E) and (F) Aeolian Dune Facies 3 (low to moderate angle wind-ripple strata); (G) Aeolian Dune Facies 4 (massive sandstone); (H) and (I) Facies AD5 (soft-sediment deformed sandstone). '1' Grainflow dominated cross-strata (up to 23°); '2' erosional truncation of dune strata (interdune migration surface); '3' wind-ripple strata; '4' millet-seed texture; '5' grainfall strata draping grainflow cross-strata (bimodal grain size); '6' reactivation surface; '7' crinkly/wavy lamination (damp interdune); '8' interfingering of dune toesets and interdune; '9' pinstripe lamination (bimodal grain size); '10' very faint grainflow dominated cross-strata (up to 23°); '11' rhizoliths (iron oxide concretion and calcite cement); '12' homogenous sediment texture with well-sorted, well-rounded and frosted grains; '13' indenter mark (vertebrate footprint); '14' soft-sediment deformed dune toesets.

accumulated where the water table was not in contact with the depositional surface, such that sedimentation was not influenced by the effects of moisture (Fryberger, 1990).

Interdune facies 2: Damp-to-wet interdune strata

Observations. Interdune Facies 2 is a laminated sandstone; laminations have low relief (several millimetres in height) and are sub-horizontal structures with irregular surfaces that are wavy-to-crinkly on a millimetre scale (Fig. 5; Kocurek & Fielder, 1982). Interdune Facies 2 is also locally associated with quasi-concentric down-folded laminations that are *ca* 300 mm in diameter (Fig. 5D). Interdune Facies 2 is commonly gradationally overlain by Interdune Facies 1 (dry interdune strata).

Interpretations. Interdune Facies 2 is interpreted to be mainly composed of adhesion strata that arose from the adhesion of moving grains to a damp surface (Hummel & Kocurek, 1984). Interdune Facies 2 accumulated on a substrate where

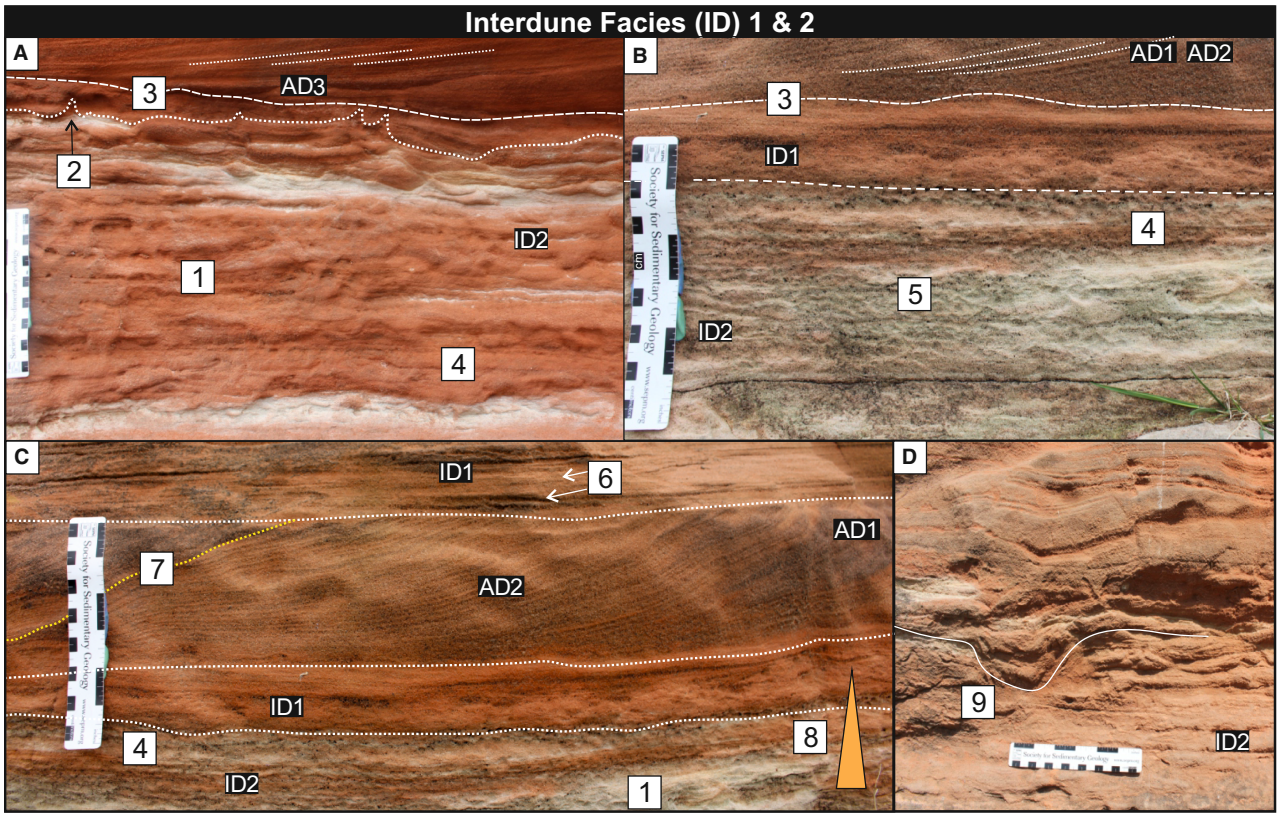

Fig. 5. Examples of aeolian interdune facies; in all images numbers denote points of interest, described below. (A) Damp interdune overlain by dune facies; (B) damp interdune, overlain by dry interdune; (C) dry interdune over- and under-lying aeolian dune facies; (D) vertebrate footprint in damp interdune. (1) Wavy or crinkly lamination; (2) small-scale flame structures; (3) textural contrast between interdune and overlying dune toesets; (4) modified wind-ripple strata; (5) adhesion ripple pseudo-lamination; (6) wind-ripple strata; (7) reactivation surface in aeolian dune set; (8) drying upwards trend (gradual transition from damp to dry interdune); (9) vertebrate footprint (indenter mark). Scale bar is 15 cm long.

the water table is close to the ground surface, such that sedimentation is influenced by the presence of moisture (Lancaster & Teller, 1988; Kocurek *et al.*, 1992). Interdune Facies 2 accumulated in interdune areas between migrating aeolian dune forms. Downfolded laminations are interpreted to be formed by vertebrate footprints (so-called indenter marks). Gradational changes between Interdune Facies 1 and Interdune Facies 2 indicate a damp-to-wet interdune transition.

In the Sherwood Sandstone Group, both dry (Interdune Facies 1) and damp (Interdune Facies 2) interdune deposits vertically and lateral transition into one another in outcrop (Fig. 5).

Fluvial facies

Detailed discussions of fluvial facies are beyond the scope of this investigation. However, summary descriptions of fluvial facies are outlined in Table 2. Fluvial facies are arranged into channelized and non-channelized architectural elements (Figs 6 and 7). Channelized fluvial architectural elements are associated with the following facies: mudclast conglomerate (FC1), planar cross-bedded sandstone (FC2), trough cross-bedded sandstone (FC3), massive sandstone (FC4), thinly laminated sandstone (FC5) and ripple cross-laminated sandstone (FC6). These facies collectively provide a record of channel-lag deposits, channel-fill deposits, and associated depositional features (cf. Picard & High, 1973; Miall, 1977; Tooth, 2000).

Non-channelized fluvial architectural elements (FP1) are expressed as horizontally and thinly laminated silty mudstones, which show alternations between siltstone and mudstone laminae (Fig. 8). This architectural element represents deposition from suspension settling in floodplains (Miall, 1977;

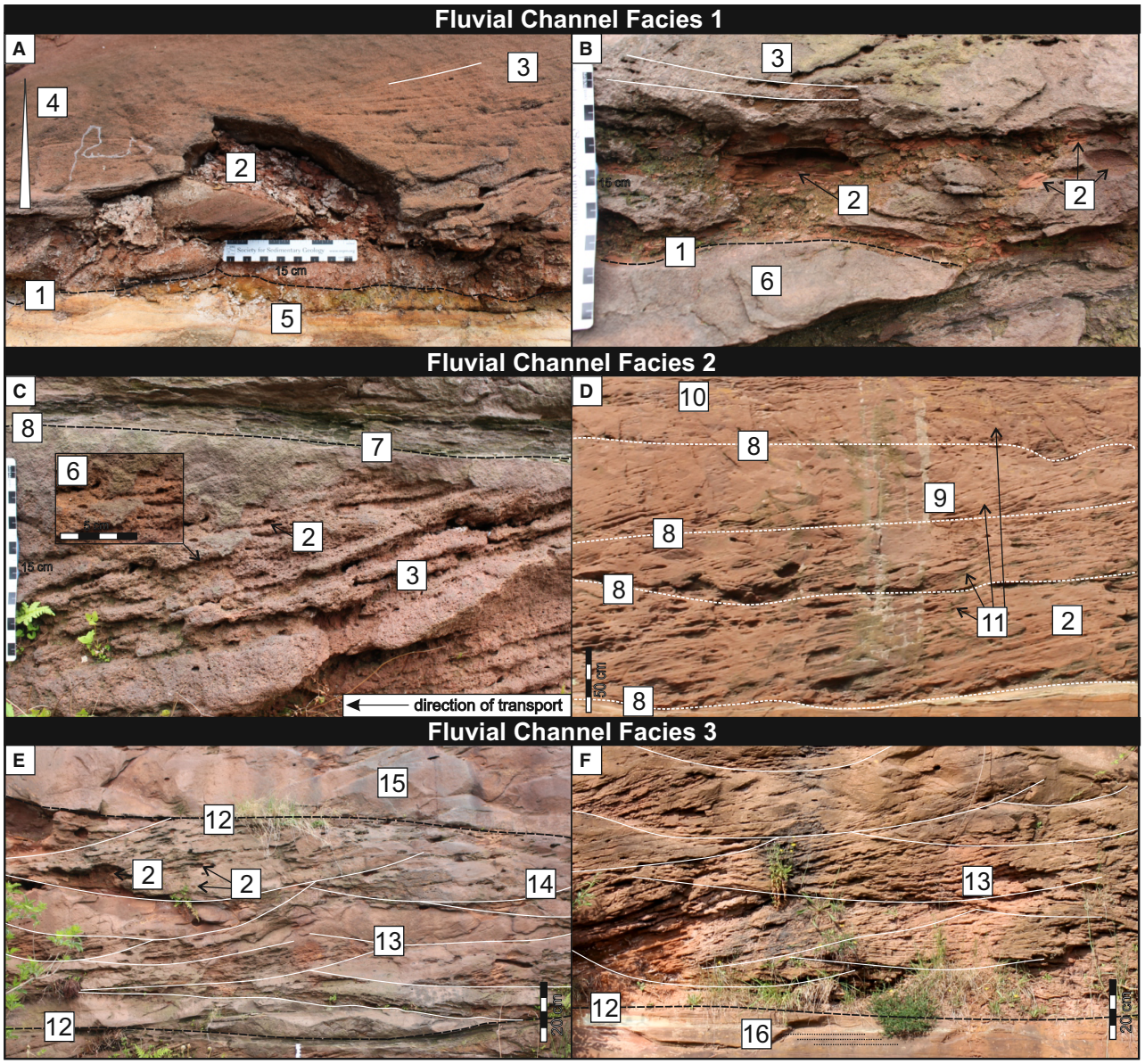

Fig. 6. Examples of fluvial channel (FC) facies; in all images numbers denote points of interest, described below. (A) and (B) Facies FC1 (mudclast conglomerate); (C) and (D) Facies FC2 (planar cross-bedded sandstone); (E) and (F) Facies FC3 (trough cross-bedded sandstone). '1' Channel base with erosional bounding surface; '2' intraformational rip-up clasts composed of laminated silty mudstone; clasts are variable in size and shape and randomly oriented; '3' cross-bedded sandstone channel-fill deposits (Facies FC2); vertical changes from facies FC1 to FC2 indicate rapid changes in flow strength; '4' fining upward sequence (normal grading); '5' wavy laminated damp interdune; '6' coarse-grained sandstone; '7' abrupt facies transitions; '8' channel element defined by basal erosional surface; '9' asymptotic foresets and toesets; '10' upper-stage plane beds; '11' multi-storey channel deposits; '12' sharp boundaries representing transitions from upper to lower flow regimes; '13' fluvial trough cross-bedding; '14' scour base; '15' massive to faintly laminated sandstone; '16' planar laminated sandstone representing waning flow stage.

Lopez & Mader, 1985) or during the final stage of channel filling and abandonment (Miall, 1977, 1978, 1988). Non-channelized fluvial facies record conditions of waning flow to form ponds and their subsequent desiccation. In places, these deposits show colour mottling that may reflect weakly developed pedoturbation over relic fluvial bedforms, in some cases with original relief partly preserved.

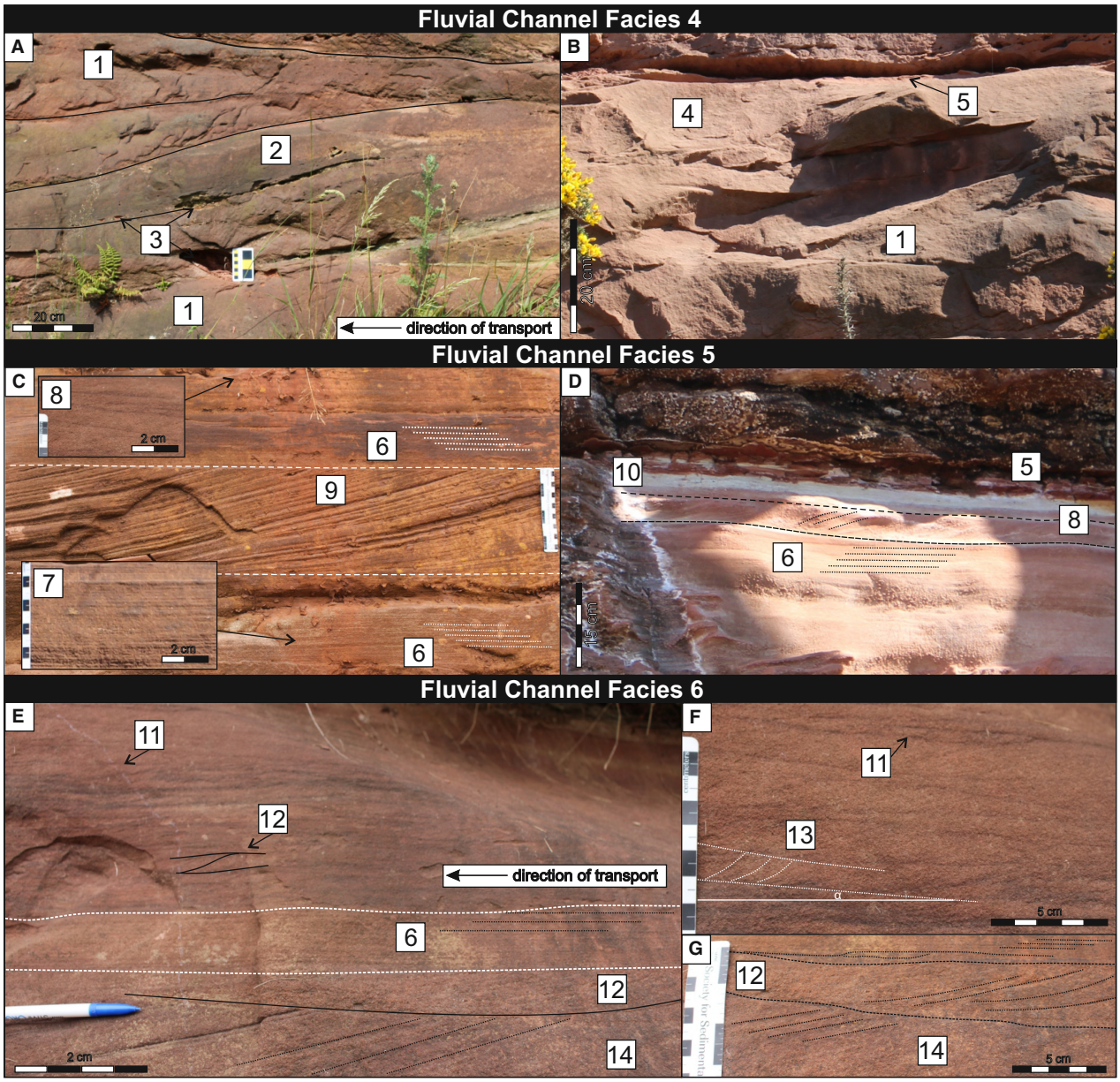

Fig. 7. Examples of fluvial channel facies; in all images numbers denote points of interest, described below. (A, B) Facies FC4 (massive structureless sandstone); (C, D) Facies FC5 (horizontally laminated sandstone); (E–G) Facies FC6 (ripple cross-laminated sandstone). (1) massively bedded sandstone lacking internal structure; (2) sigmoidal foresets; (3) mud-clast conglomerates; (4) homogenous stacked sets; (5) silty mudstones; (6) planar (horizontal) laminated sandstone; (7) bimodal grainsize; (8) lower flow regimes; (9) low angle inclined fluvial cross-beds; (10) normal grading displaying current (ripple) laminated sandstone at the top; (11) fine-grained sand with waning-flow mud drapes; (12) critical to supercritical climbing ripples (indicative of episodes of high sediment flux and waning flow conditions to enable rapid accumulation); (13) subcritical climbing-ripple stratification; (14) inclined fluvial cross-bed set. Scale bar is 15 cm long.

Depositional setting

Analysis of contemporary ergs has provided crucial insights into the distinctive aeolian architecture found in central and marginal dune-field areas (e.g. Al-Masrahy & Mountney, 2013). Notably, the dimensions and connectivity of interdune corridors exhibit a consistent pattern, with an increase in width, length and

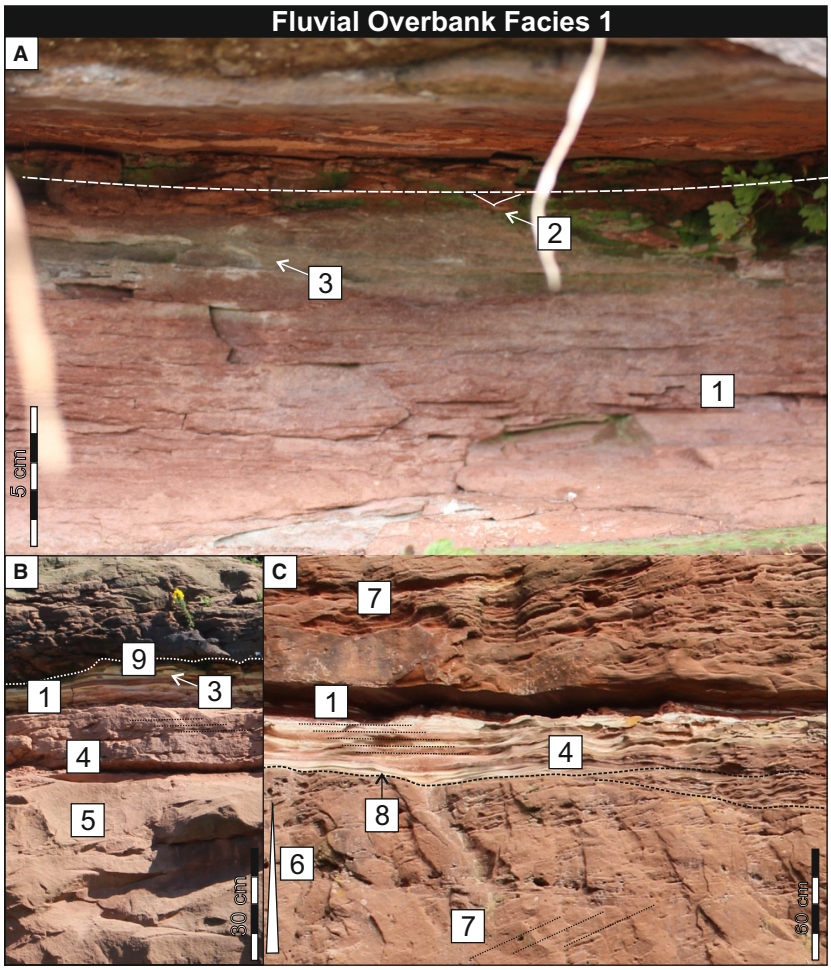

Fig. 8. Examples of fluvial overbank facies; in all images numbers denote points of interest, described below. (A) to (C) Facies FO1 (horizontally laminated thin-bedded silty mudstone). '1' Planar, thinly laminated, laterally extensive silty mudstone; '2' desiccation cracks in the top of mudstone horizon; '3' colour mottling (streaks); '4' channel-fill waning deposits; '5' massive fluvial deposits (Facies FC4); '6' normal grading; '7' fluvial channel-fill deposits; '8' abrupt channel abandonment; '9' fluvial channel scour surface.

interconnection from the central region towards the margin, corresponding to the reduction in neighbouring dune size (Al-Masrahy & Mountney, 2013). In marginal erg environments, aeolian systems often interact with fluvial landforms, to varying extents. In contrast, central erg settings predominantly feature aeolian landforms with limited interaction with non-aeolian elements. These contemporary observations serve as a valuable framework for interpreting ancient geological records (cf. Mountney & Jagger, 2004; Hême de Lacotte & Mountney, 2022). A marginal-erg setting for the Sherwood Sandstone Group is demonstrated by Thompson (1970a,b) and Mountney & Thompson (2002). This inference is supported by the presence of contemporaneous aeolian and fluvial environments, which interdigitate laterally and vertically in the stratigraphic record (cf. Jones & Blakey, 1997; Herries, 1993; Figs 9 to 12). The presence of locally interconnected damp-to-wet interdunes in the Sherwood Sandstone Group (Fig. 10) aligns with observations of increased connectivity of interdunes towards erg margins in the modern and ancient record (Mountney & Jagger, 2004; Taggart *et al.*, 2010; Al-Masrahy & Mountney, 2013).

Quantitative analysis

Deposits of the Wilmslow Sandstone Formation and Helsby Sandstone Formation in the Sherwood Sandstone Group have been compared with literature case studies from DASA based on: (i) climatic conditions (the Sherwood Sandstone Group was deposited under a greenhouse climate); (ii) age (the studied interval of the Sherwood Sandstone Group is Mesozoic); (iii) dune physiographic setting (the studied interval of the Sherwood Sandstone Group is interpreted to have been deposited in a marginal dune field setting; Mountney & Thompson, 2002); (iv) basin setting (the Sherwood Sandstone Group was deposited in a rift basin); and (v) aeolian system

Table 2. Summary information outlining the fluvial facies associations in the Sherwood Sandstone Group.

Fluvial Lithofacies

Facies	Colour	Grain-Size	Thickness	Texture	Facies Characteristics	Occurrence	Architectural Element
FC1: Intra/ Extra-formational mudclast conglomerate	Reddish-brown	Clasts vary in size from 10 to 200 mm	Set thickness = 0.1 –0.3 m	Clast supported; poorly sorted; angular to rounded-bladed	Massively to crudely bedded. Thinly laminated mudstone and silty mudstone as rip-up clasts	Channel lag (common)	Fluvial Channel
FC2: Planar cross-bedded sandstone	Reddish-brown to light brown	Fine to very coarse-grained	Set thickness = 0.2 –1.0 m; stacked cosets = 2.5 m	Moderate to poorly sorted; sub-rounded	Planar cross-bedded sandstone; contained in channelized elements defined by basal erosion surfaces; cross-bedding shows asymptotic foresets and toesets. Sets are stacked and have sharp boundaries; mud clasts are present as lag deposits	Channel fill (common)	Fluvial Channel
FC3: Trough cross-bedded sandstone	Reddish-brown to light brown	Fine to very coarse-grained	Set thickness = 0.1 –0.3 m; coset thickness = 1 –2 m	Moderate to poorly sorted; sub-rounded to angular	Fluvial trough cross-beds; mud clasts (lag deposits); representing lower flow regimes	Channel fill (common)	Fluvial Channel
FC4: Massive (structureless) sandstone	Brown and light brown	Fine to medium-grained	Set thickness = 0.1 –3.0 m	Moderate to well-sorted; rounded to sub-rounded	Homogeneous stacked sets; absence of internal structure (massively bedded)	Channel fill (common)	Fluvial Channel
FC5: Horizontally laminated sandstone	Brown and pinkish-brown	Very fine to medium grained	Set thickness = 0.2 –0.6 m; lamination thickness = 1 –5 mm	Moderate to well-sorted; sub-rounded to sub-angular	Planar (horizontal) laminated sandstone. Homogeneous grain size; faint flat lamination due to well-sorted nature of grains; bimodal grain-size distribution; sets fine upward, with current (ripple) laminated sandstone towards the top	Upper channel fill (common)	Fluvial Channel/ Floodplain
FC6: Ripple cross-laminated sandstone	Brown to reddish-brown	Very fine to coarse-grained	Set thickness = 0.1 –0.3 m	Moderate to poorly sorted; sub-rounded to angular	Mud-draped climbing ripples and lenticular bedding; complete preservation of ripple forms in places	Top channel fill (rare)	Fluvial Channel/ Floodplain
FC7: Dewatered convoluted sandstone		Fine to medium-grained	Set thickness 0.1 –0.6 m	Moderate to well-sorted; rounded to sub-rounded	Convoluted strata include slump and water-escape structures	Channel fill (rare)	Fluvial Channel/ Floodplain

Table 2. (continued)

Facies	Colour	Grain-Size	Thickness	Texture	Facies Characteristics	Occurrence	Architectural Element
Fluvial Lithofacies							
FP1: Horizontally thin-laminated silty mudstone	Red, brown, white	Mudstone to siltstone	Set thickness 0.1 –0.3 m	Moderate to well-sorted; sub-rounded	Thinly laminated, laterally extensive, sets rarely exceeding 30 cm in thickness; it commonly exhibits a white or mottled greenish-white appearance; desiccation cracks may be preserved at the top of the mudstone	Overbank areas (common)	Floodplain

type (the studied interval of the Sherwood Sandstone Group was deposited in a water-table-influenced aeolian system). The results of this analysis are presented in Table 2 and discussed below; for the number of readings associated with all quantitative analyses, refer to Table 2.

Dune-sets (Fig. 13) of the Sherwood Sandstone Group (mean thickness = 0.92 m) are on average significantly thinner than those from: (i) case studies included in DASA generally (mean = 5.19 m); (ii) greenhouse systems (mean = 6.13 m); (iii) rift basin systems (mean = 2.3 m); and (iv) Mesozoic systems (mean = 7.72 m). There is no significant difference between the average thickness of the dune-set elements of the Sherwood Sandstone Group and the average set thickness of: (i) wet aeolian systems (mean = 2.81 m); and (ii) marginal aeolian systems (mean = 2.24 m).

Dry-interdune deposits (Fig. 13) of the Sherwood Sandstone Group (mean thickness = 0.3 m) are on average significantly thinner than: (i) all systems in DASA (mean = 1.59 m); (ii) greenhouse systems (mean = 2.21 m); and (iii) Mesozoic systems (mean = 2.06 m). There is no significant difference between the mean thickness of the dry-interdune strata of the Sherwood Sandstone Group and that of dry-interdune elements from: (i) rift basin systems (mean = 1.12 m); (ii) wet aeolian systems (mean = 1.1 m); and (iii) marginal aeolian systems (mean = 0.85 m).

Wet-interdune deposits of the Sherwood Sandstone Group (Fig. 13) (mean thickness = 0.29 m) are on average significantly thinner than: (i) all systems in DASA (mean = 1.27 m); (ii) greenhouse systems (mean = 1.63 m); (iii) marginal aeolian systems (mean = 0.41 m); and (iv) Mesozoic systems (mean = 4.91 m). There is no significant difference between the mean thickness of the wet-interdune strata of the Sherwood Sandstone Group and that of wet-interdune elements from: (i) rift basin systems (mean = 1.27 m); and (ii) wet aeolian systems (mean = 1.17 m).

Relationships between the length and thickness of all architectural elements are presented graphically in Fig. 14. The deposits of the Sherwood Sandstone Group are on average thinner and shorter than architectural elements from most DASA examples. However, the relationships between the length and thickness of dune and interdune deposits of the Sherwood Sandstone Group closely resemble those of rift-basin fills.

Regarding facies associated with sets of aeolian dune origin, a greater proportion of

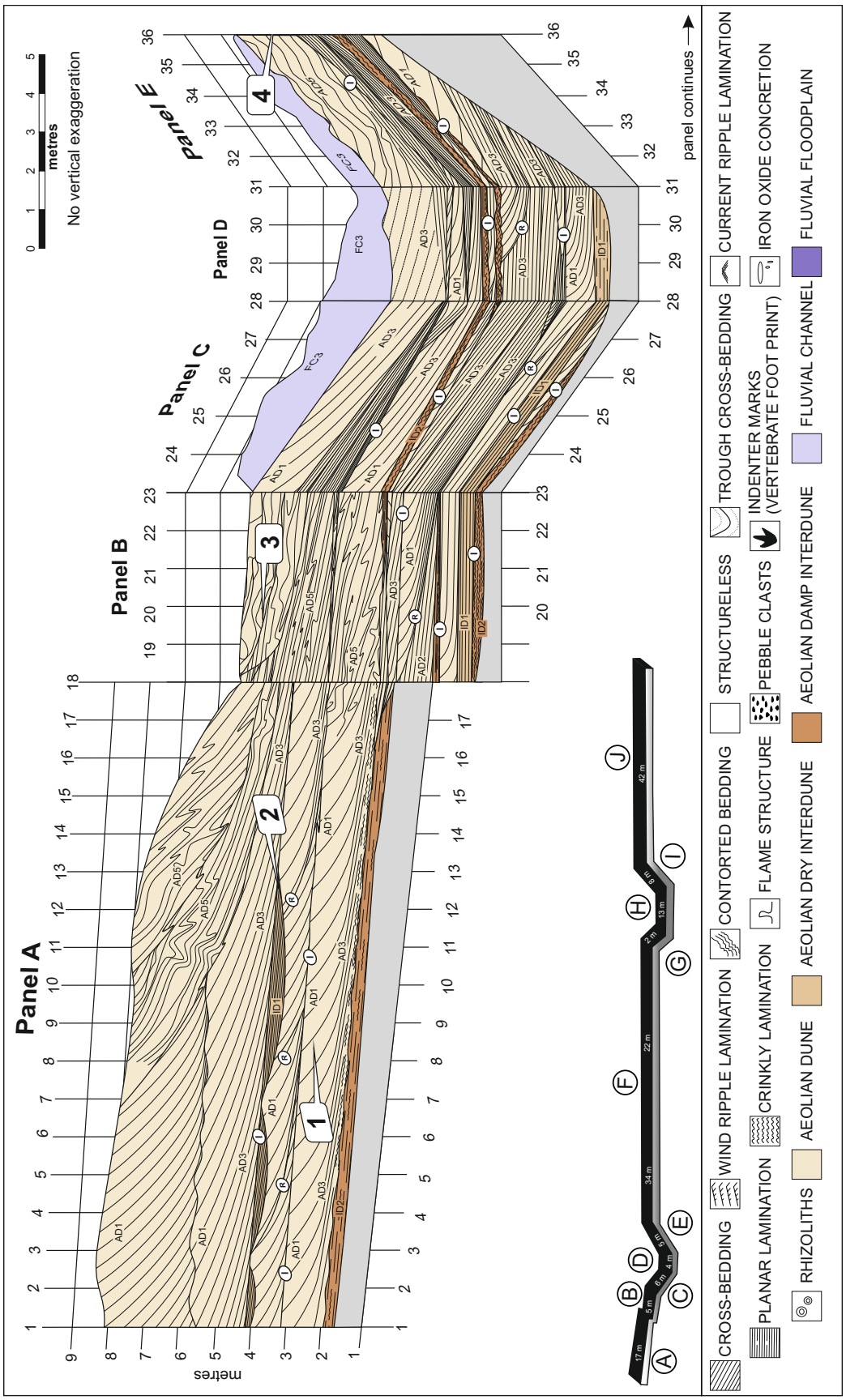

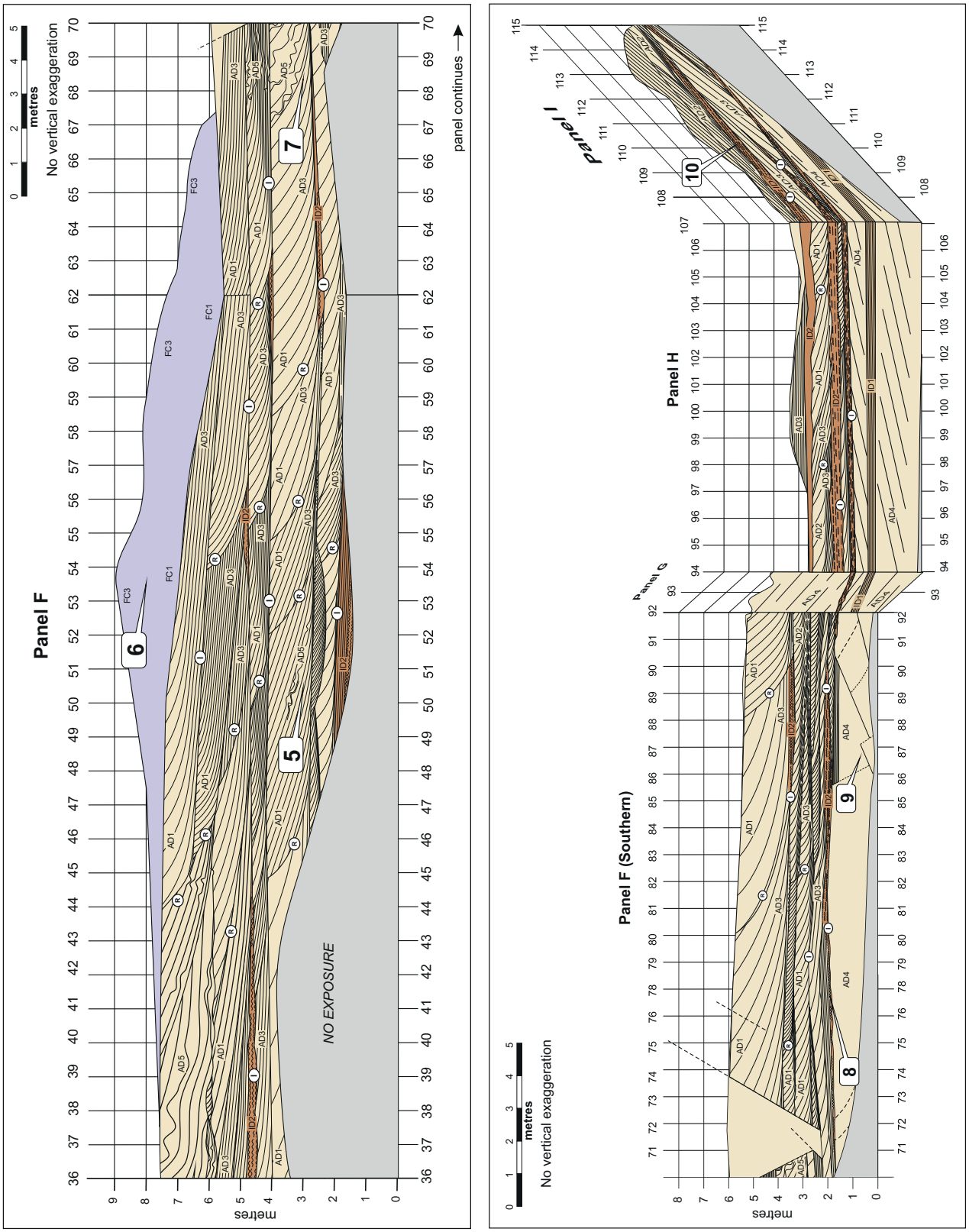

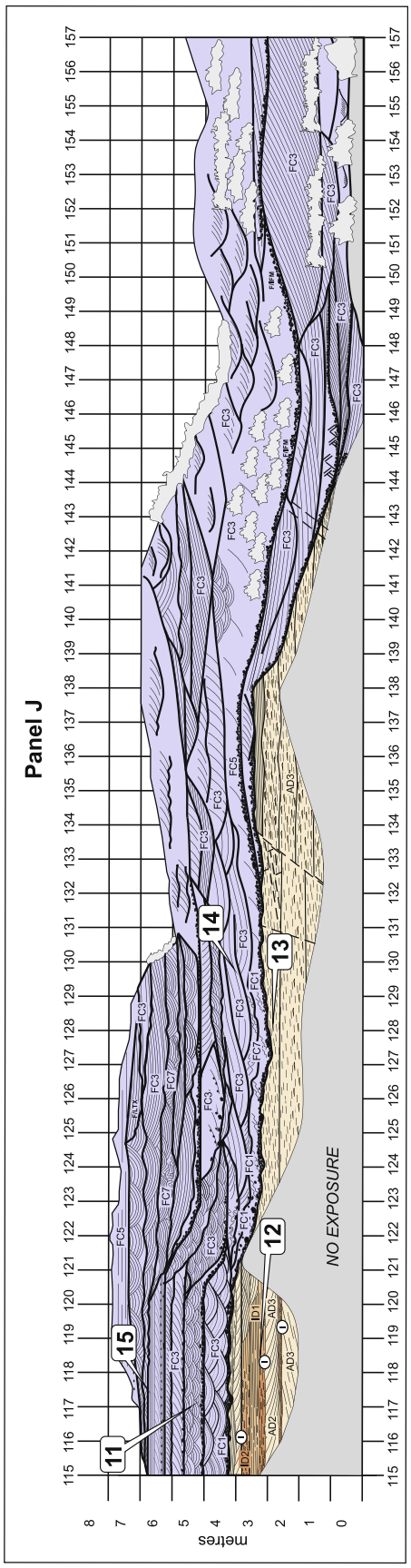

Fig. 9. Architectural panels of the Beacon Hill outcrop. Numbers denote points of interest outlined below: '1' Medium-grained sandstone characterized by high-angle aeolian grainflow strata (Aeolian Facies (AD) 1). Grainflow deposits 50 mm thick. '2' Medium-grained sandstone characterized by planar and wind-ripple strata (dry interdune; Interdune Facies (ID) 1). '3' Thick convoluted aeolian dune facies (Aeolian Dune Facies (AD) 5). '4' Medium-grained grainflow dominated sandstone with small-scale slump structures. '6' Channelized fluvial successions cut into aeolian successions. '7' Medium to coarse grained sandstone of thick convoluted aeolian-dune sets. '8' Lateral transitional facies change from wet-interdune to wind-ripple strata indicative of accumulation on a dry substrate. '9' Faulted blocks due to regional tectonic movements. '10' Wet interdune element dominated by wavy laminated, very fine-grained sandstones that extend laterally more than 20 m. '11' Small-scale fluvial trough cross-beds associated with intraformational clasts. '12' Very fine-grained planar to wavy laminated sandstone of wet and dry interdune elements due to water table fluctuations. '13' Major fluvial incursion into an aeolian sandsheet succession that is dominated by wind-ripple strata. Extraformational and intraformational clasts associated with erosional base of fluvial channel. '14' Large-scale, wedge-shaped sets of trough cross-bedded, medium to coarse-grained sandstone (3 m wide). '15' Fluvial horizontal laminated sets characterized by medium-grained sandstone channel-fill elements.

recorded facies types in the Sherwood Sandstone Group (78%) is formed by grainflow facies compared with all other quantitative outputs. These include deposits associated with greenhouse conditions, rift basins, wet aeolian systems, marginal aeolian systems and Mesozoic-age aeolian systems (Fig. 15). Windripple facies form a lesser proportion of the recorded facies types in the Sherwood Sandstone Group (9%) compared with all other quantitative outputs (Fig. 15).

DISCUSSION

Aeolian architecture

Aeolian dunes and interdunes may cover an accumulation surface to varying extents; both can potentially climb as they migrate to leave a stratigraphic record. Understanding how and when dune and interdune elements of different sizes and types ultimately become preserved in the stratigraphic record is key to interpreting the environmental significance of preserved aeolian successions. The preserved aeolian architecture of the Sherwood Sandstone Group is characterized dominantly by wet-to-damp and dry interdune elements that separate aeolian dune sets.

Aeolian dune sets

The thickness of aeolian dune sets is determined by: (i) the angle of bedform climb; and (ii) the wavelength (size) of the formative dune. The latter is itself governed by the availability and supply of sand for the construction of dunes, and the transport capacity of the wind and its flow behaviour (Lancaster & Teller, 1988, Lancaster, 1992; Kocurek & Lancaster, 1999). For dunes and interdunes of a given size, greater angles of bedform climb – induced by either a more rapid rise in the level of the accumulation surface (for example in response to water-table rise) or slower rates of bedform migration – will result in the preservation of thicker dune and interdune sets in the geological record. For a given angle of climb, larger dune wavelengths will result in thicker dune sets in the geological record.

Preserved dune sets of the Sherwood Sandstone Group are significantly thinner than those of all other aeolian systems recorded in DASA and tested in this investigation, except for dune-sets of dune-field (erg) margins (Fig. 13). Given that the thickness of preserved dune-sets is governed by dune wavelength and angle of climb, this suggests that the Sherwood Sandstone Group was associated with relatively small formative dunes, a low angle of climb, or a combination of both. This observation is discussed below.

Modern aeolian systems are often characterized by predictable changes in dune type from the central regions of dune fields to their margins (e.g. Great Sand Dunes of Colorado, USA; Rub' Al Khali, Saudi Arabia). Larger, more closely spaced dunes tend to characterize dune-field centres, whereas smaller dunes with relatively wide interdune flats tend to characterize dune-field margins (Andrews, 1981; Al-Masrahy & Mountney, 2013). Given that the successions of the Sherwood Sandstone Group are interpreted as a series of water table-controlled aeolian-dominated erg-margin systems (*sensu* Mountney & Jagger, 2004; see Section '*Depositional Setting*' for a full discussion of erg-margin setting), the size of the formative dunes in the Sherwood Sandstone Group may have been a primary control on preserved dune-set thickness. Mountney & Thompson (2002) reconstruct dune wavelengths in the Sherwood Sandstone Group of between *ca* 12 to 40 m, lateral spacing of *ca* 15 to 46 m, and amplitudes of *ca* 5 m; the formative dunes of the Sherwood Sandstone Group were relatively small compared to modern sinuous-crested dunes (Wilson, 1973). The inference of small formative dunes is supported by the arrangement of facies within aeolian dune sets of the Sherwood Sandstone Group. Typically, small dunes migrate relatively rapidly (e.g. Yang *et al.*, 2021) and such forms generally do not have broad, low-angle inclined plinths; this results in the preservation of lee-slope deposits that comprise of a relatively larger fraction of grainflow strata and relatively less windripple strata (Romain & Mountney, 2014). In the Sherwood Sandstone Group, grainflow strata form a greater proportion of recorded facies types in dune-set elements (78%; Fig. 15), relative to other dune sets recorded in DASA (<13%; Fig. 15); this is common for dunes where grainflow strata that extend close to the base of lee slopes, and for and preserved dune sets (cf. Hunter, 1977a; Romain & Mountney, 2014; Nield *et al.*, 2017). In addition, interdune geometries – the shape of which is governed by the morphological arrangement and spacing of adjacent dunes – support an inference of relatively small formative dunes. Interdunes with lenticular plan

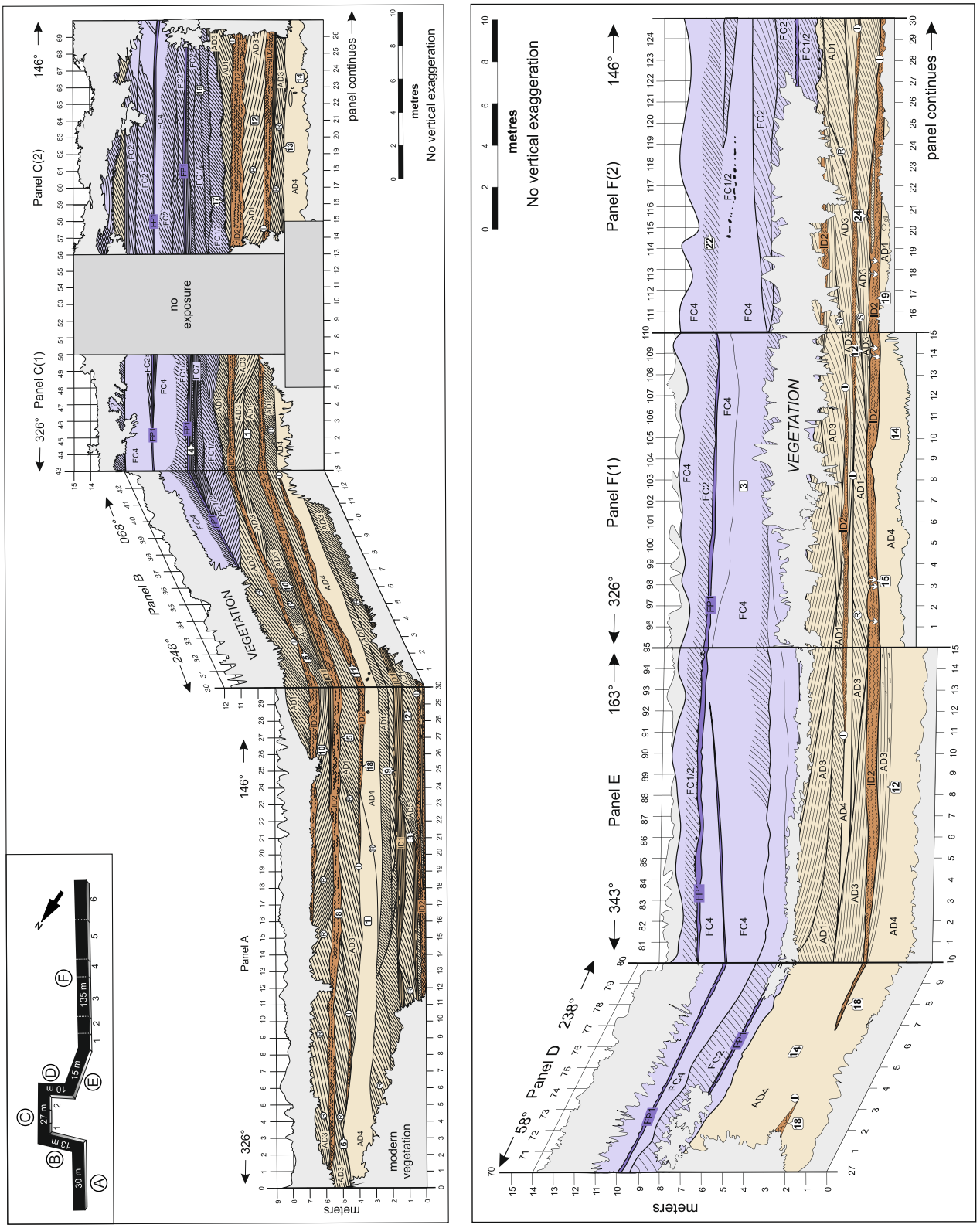

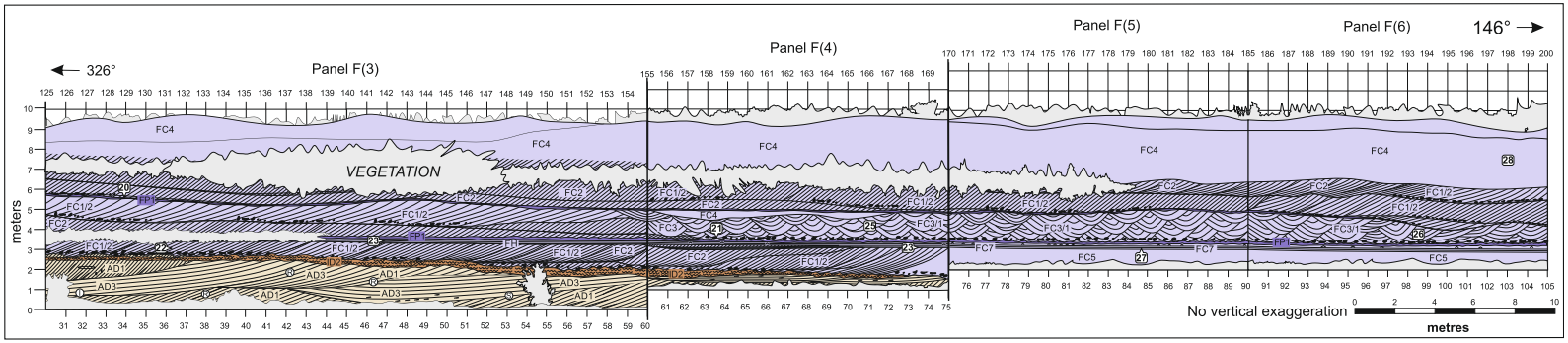

Fig. 10. Architectural panels of the Runcorn Road Cut outcrop. Numbers denote points of interest outlined below: '1' Stacked aeolian dune-strata separated by interdune surface. '2' Moderate-high angle aeolian dune foresets (grainflow dominated), pinching out towards the base of lee-slope. '3' Dune toe-set soft-sediment deformation, laterally intertonguing with damp interdune strata. '4' Fluvial faint flat lamination; homogenous grain size due to well-sorted nature of grains. '5' Dune strata with erosional truncation surface; deflation surface. '6' Downwind-dipping reactivation surfaces. '7' Spatially isolated damp interdune unit. '8' Damp interdune unit showing erosional topography on both upper and lower surface; pinches out laterally. '9' Medium to coarse-grained sandstone dominated by planar and wind-ripple laminated of dry interdune strata. '10' Lateral transition from crinkly-wavy laminated (damp) to wind-ripple (dry) interdune strata. '11' Lateral thickening of wavy laminated interdune horizon. The corresponding legend is provided in Fig. 9.

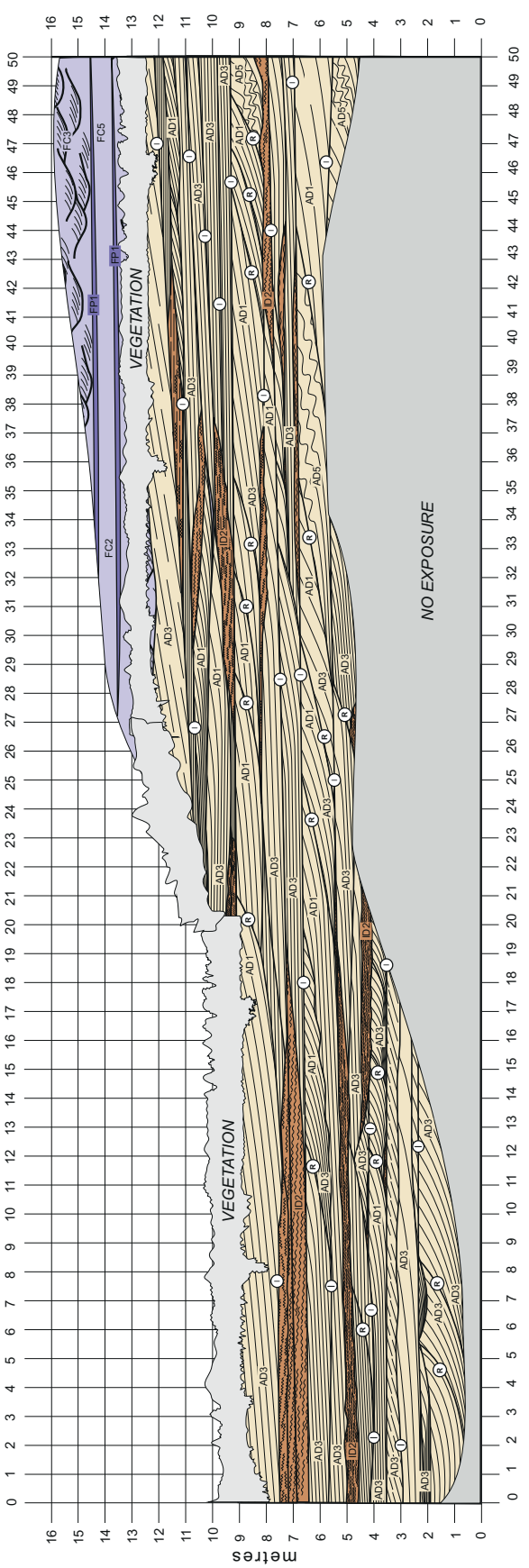

Fig. 11. Architectural panels of the Dunsdale Hollow outcrop. Numbers denote points of interest outlined below: '1' Stacked beds of wet interdune origin dominated by wavy laminated, very fine-grained sandstones that extend laterally more than 13 m. Indicates cyclic deposition within interdune depressions. '2' Fine-grained sandstone dominated by planar and wind-ripple laminated sandstone; dry interdunes. '3' Aeolian grainflow strata characterized by high-angle stratified, medium-grained sandstone. Grainflow deposits are each up to 60 mm thick. '4' Erosive base of aeolian dune dominated by grainflow strata. '5' Lateral transitional facies change from wet interdune to wind-ripple strata indicative of dry interdune. '6' Lateral thinning wet-interdune facies element. '7' Stacked aeolian dune strata separated by interdune surface. The corresponding legend is provided in Fig. 9.

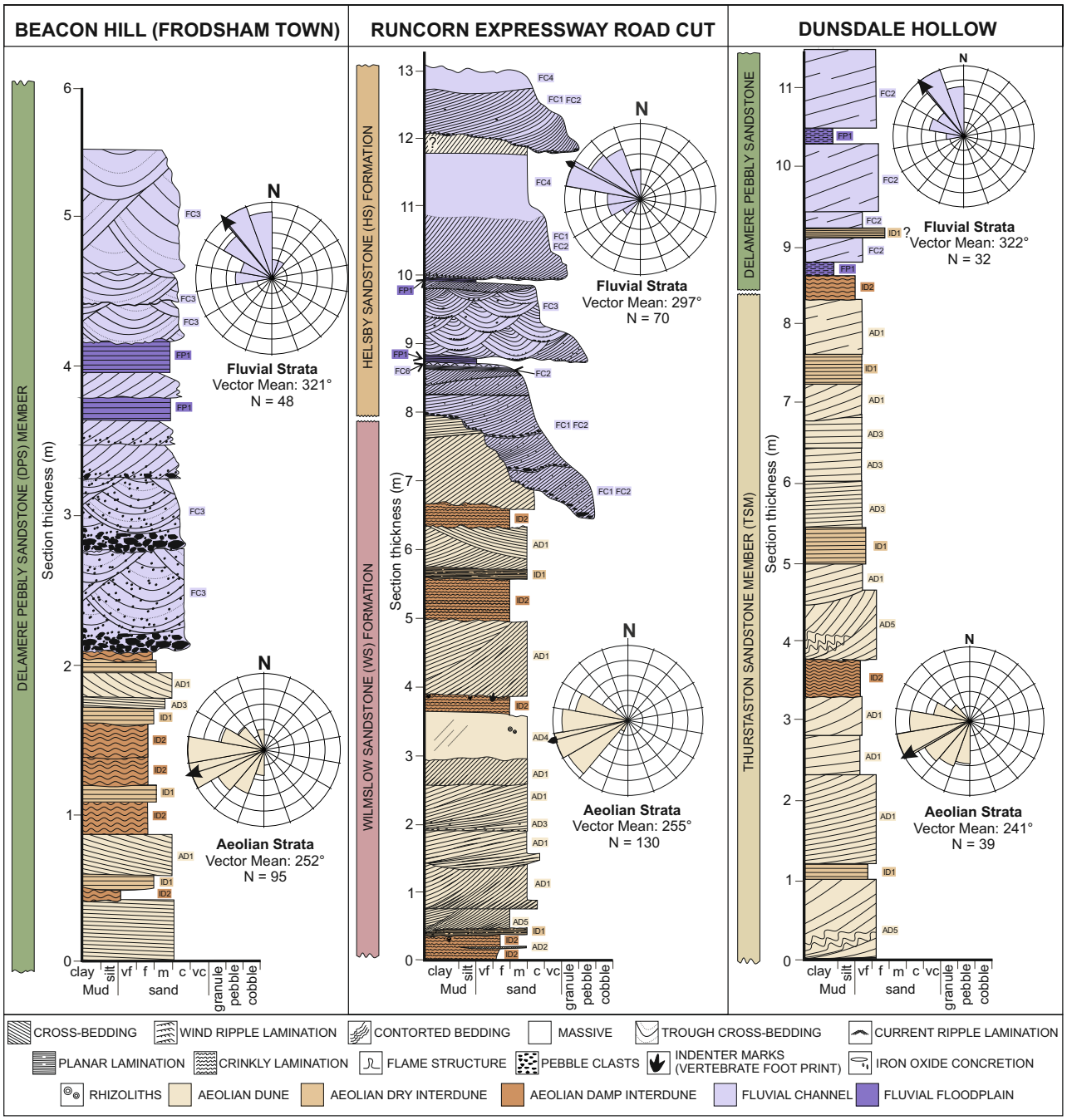

Fig. 12. Representative logs and associated palaeocurrent data for the studied outcrops. *N* = number of readings. Latitude and longitude of logs as follows: Beacon Hill = 53.33°N, 2.74°W; Runcorn Expressway = 53.22°N, 2.73°W; Dunsdale Hollow = 53.28°N, 2.73°W.

forms are commonly associated with small, rapidly migrating transverse or oblique, sinuous-crested barchanoid dunes, between which isolated interdune depressions are present (e.g. Carruthers, 1987; Rubin, 1987; Lancaster, 1995). The resultant preserved geometry of the interdune architectural elements may also be controlled by changes in the angle of climb during dune-interdune migration (Mountney, 2012).

The small size of the dunes also likely influenced the angle of climb of the system. Notably,

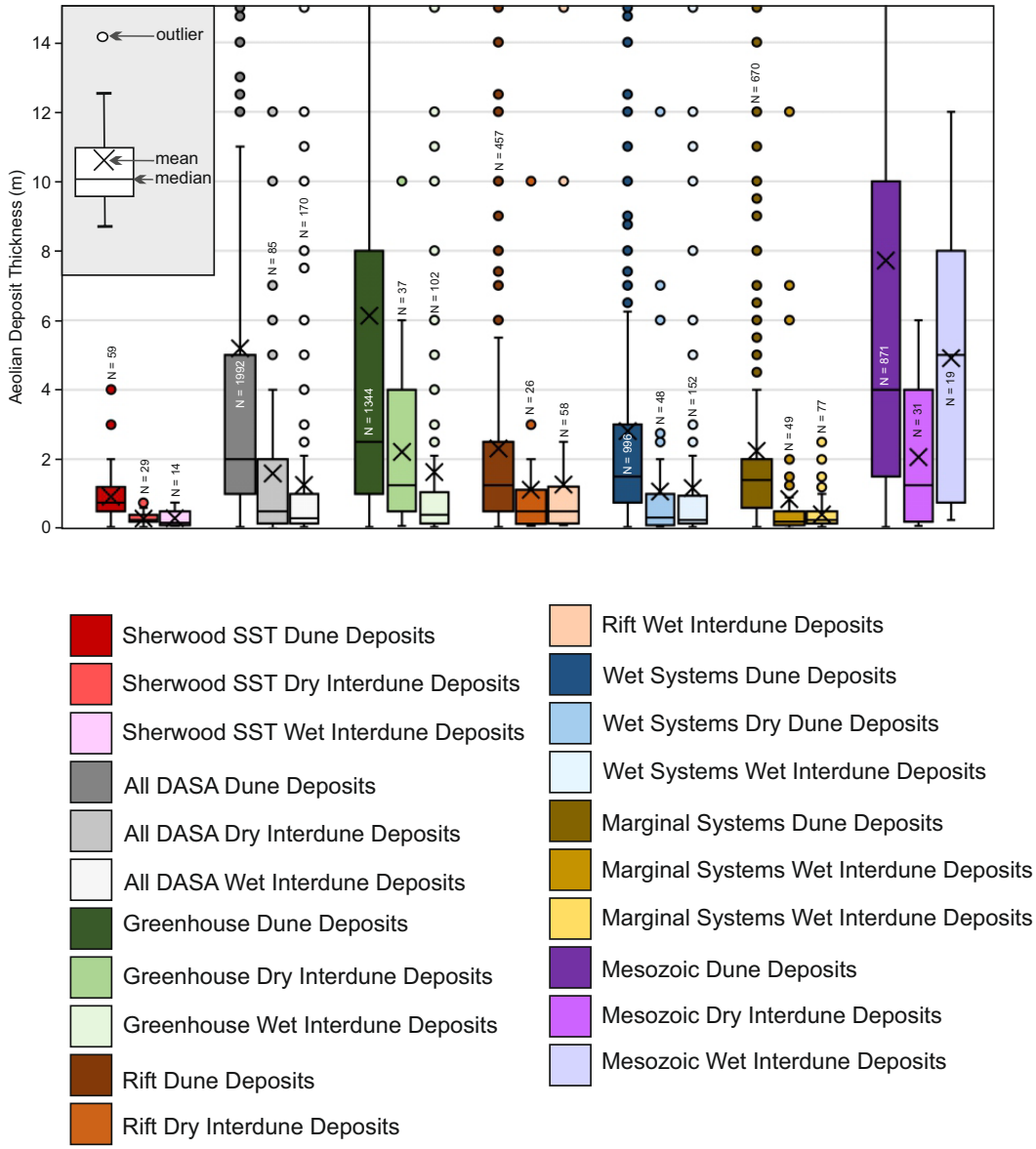

Fig. 13. Box and whisker plots showing the thickness of various aeolian architectural elements in the Sherwood Sandstone Group compared with database outputs.

dune migration rates tend to be scaled with bedform size, such that smaller bedforms have faster rates of horizontal migration relative to larger bedforms (Bagnold, 1941; Hersen *et al.*, 2002; Groh *et al.*, 2008). However, migration rates of dunes can also be influenced by multiple other factors, including: (i) the number of dunes per unit surface area; (ii) wind intensity; (iii) grain size; (iv) dune shape; (v) topography; (vi) precipitation and water-table level; and (vii) vegetative cover (Bogle *et al.*, 2015; Boulghobra, 2016; Hamdan *et al.*, 2016; Yang *et al.*, 2019). A faster dune migration rate (associated with a smaller dune size) will result in a lower angle of climb (Mountney & Thompson, 2002), for a given rate of accumulation (i.e. rate of accumulation-surface rise).

The relatively small size of formative dunes in the dune-field margin setting of the Sherwood Sandstone Group systems may have also been influenced by the relative wetness of the depositional surface. Elevated water tables and wet substrates in the Sherwood Sandstone Group are indicated by the prevalence of damp and wet

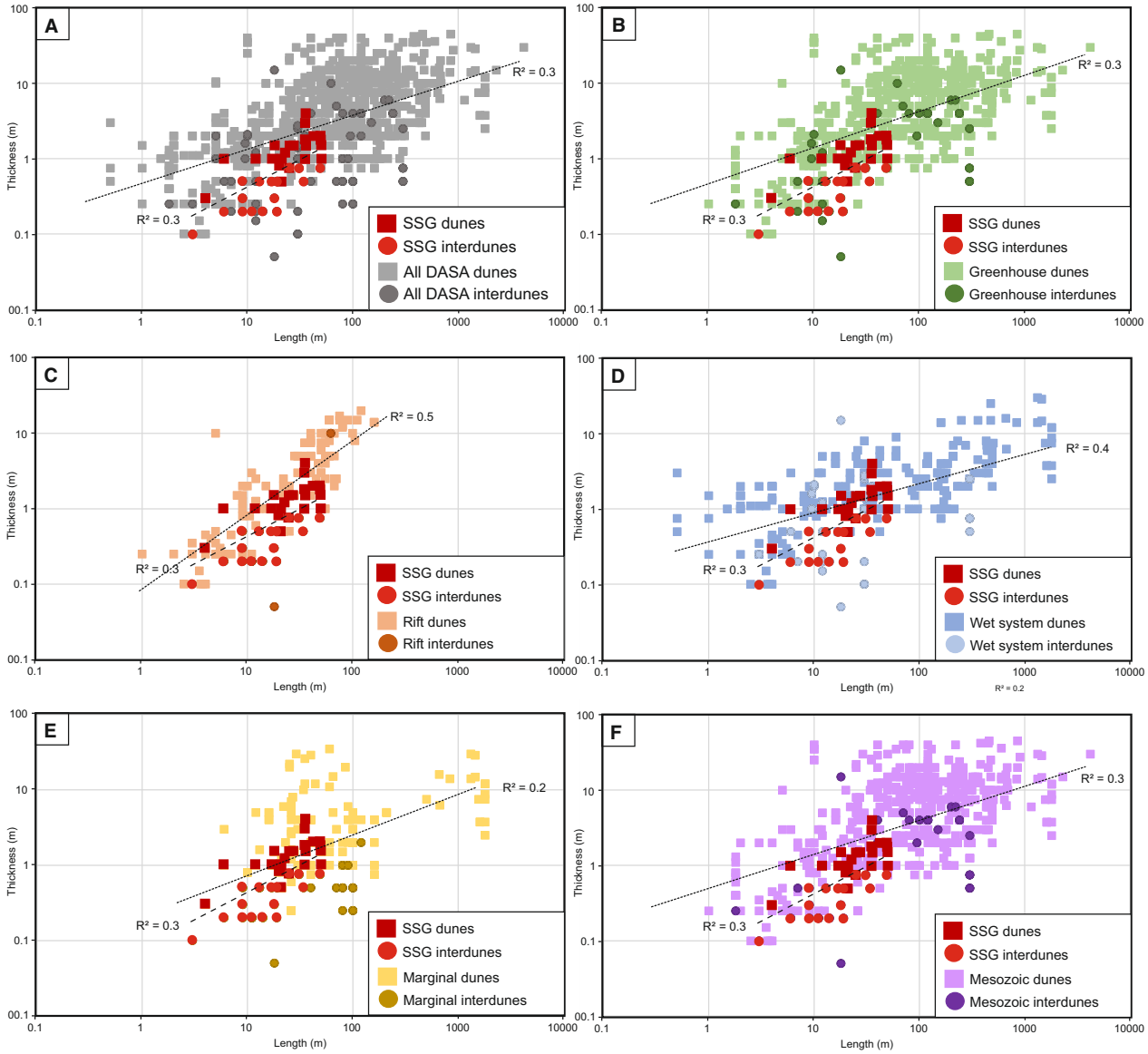

Fig. 14. Comparison of the relationship between the length (maximum recorded or observed lateral extent of architectural element in orientation parallel to inferred direction of dune migration) and thickness of architectural elements in the Sherwood Sandstone Group with various database outputs.

interdunes (Figs 5 and 9 to 12). These conditions act to limit the availability of sediment for dune construction (Kocurek, 1981a; Hotta *et al.*, 1984; Granja *et al.*, 2008; Mountney & Russell, 2009), as higher moisture levels at the surface act to bind sediment particles and retard aeolian transport (e.g. McKenna-Neuman & Nickling, 1989; Sherman, 1990; Scheidt *et al.*, 2010). As such, a high water table may have acted to limit the size to which dunes could grow. The wetness of the depositional surface may be intimately tied to the marginal setting of the Sherwood Sandstone Group. In modern aeolian systems water-table levels commonly vary spatially from dune-field margins to their centres, because pathways of ephemeral floodwaters are controlled by aeolian topography and because erg margins are closer to areas of direct groundwater recharge (e.g. Yang *et al.*, 2010). Larger and relatively open (i.e. interconnected) interdune flats tend to allow the penetration of fluvial floods considerable distances into dune

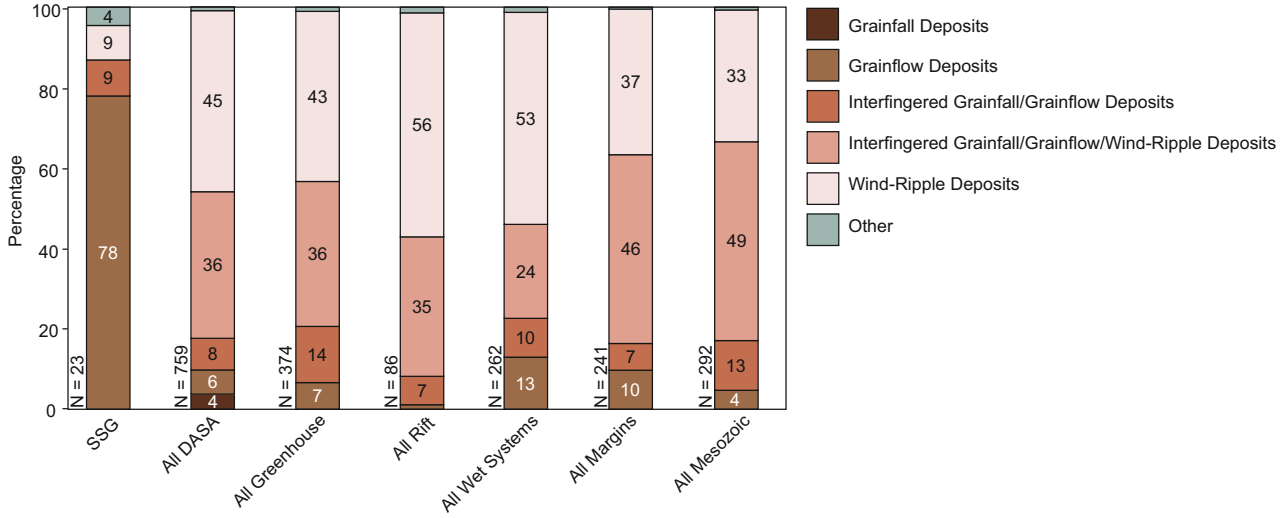

Fig. 15. Proportions of facies within the dune sets of the Sherwood Sandstone Group and database outputs.

fields, in some circumstances (Al-Masrahy & Mountney, 2015). Such streamflow incursions may occur periodically, in some cases in response to seasonal recurrence of rainfall run-off; these events can wet the depositional surface and recharge groundwater aquifers, leading to an absolute rise in the water table.

Models of wet system development

The preserved aeolian successions of the Sherwood Sandstone Group are characterized by an abundance of damp to wet-interdune elements that separate aeolian dune sets. The sedimentary architecture of these interdune deposits indicates that the water table was at the level of the depositional surface, or close to it during accumulation. The presence of an elevated water table in a so-called wet aeolian system means that aeolian bedform construction might have been supply and/or availability limited (Kocurek & Lancaster, 1999), whereas the potential for the accumulation of thick interdune flats (damp or wet) separating the downwind climbing dune strata was high (Hummel & Kocurek, 1984; Mountney & Jagger, 2004).

In wet aeolian systems, accumulation can occur according to two end-member styles: climbing (e.g. Crabaugh & Kocurek, 1993; Kocurek & Havholm, 1993; Carr-Crabaugh & Kocurek, 1998) and non-climbing accumulation (e.g. Simpson & Loope, 1985; Loope & Simpson, 1992). See '*Background*' for a discussion of these accumulation styles. The sedimentary architecture of the wet-interdune deposits of the Sherwood Sandstone Group suggests that accumulation occurred via both of these mechanisms. Climbing accumulation in the Sherwood Sandstone Group is indicated by the interton-guing of dune toesets (Aeolian Dune Facies 1 [mixed grainflow and wind-ripple strata] and Aeolian Dune Facies 3 [wind-ripple strata]) with strata in the adjacent interdunes (Interdune Facies 1 [dry interdune strata] and Interdune Facies 2 [damp-to-wet interdune strata]), suggesting that interdune deposition was synchronous with dune migration and accumulation (cf. Pulvertaft, 1985; Loope & Simpson, 1992; Kocurek & Havholm, 1993; Mountney & Thompson, 2002; Fig. 16). However, in other places, non-climbing accumulation is indicated by the contacts between interdune and dune deposits, which display sharp, erosional surfaces (Fig. 16). This suggests that episodic minor water-table falls may have allowed wind reworking of the upper portions of interdune units.

If both climbing and non-climbing accumulation mechanisms are invoked to explain the architecture of the wet-interdune deposits of the Sherwood Sandstone Group, the angles of climb must have fluctuated between positive and negative values. Angles of climb can vary according to the rate of accommodation generation, the rate of water-table rise and the rate of dune migration (Mountney & Thompson, 2002). The wet-interdune deposits of the Sherwood Sandstone Group have similar thickness statistics to the interdune deposits of other successions from rift basins and wet aeolian systems

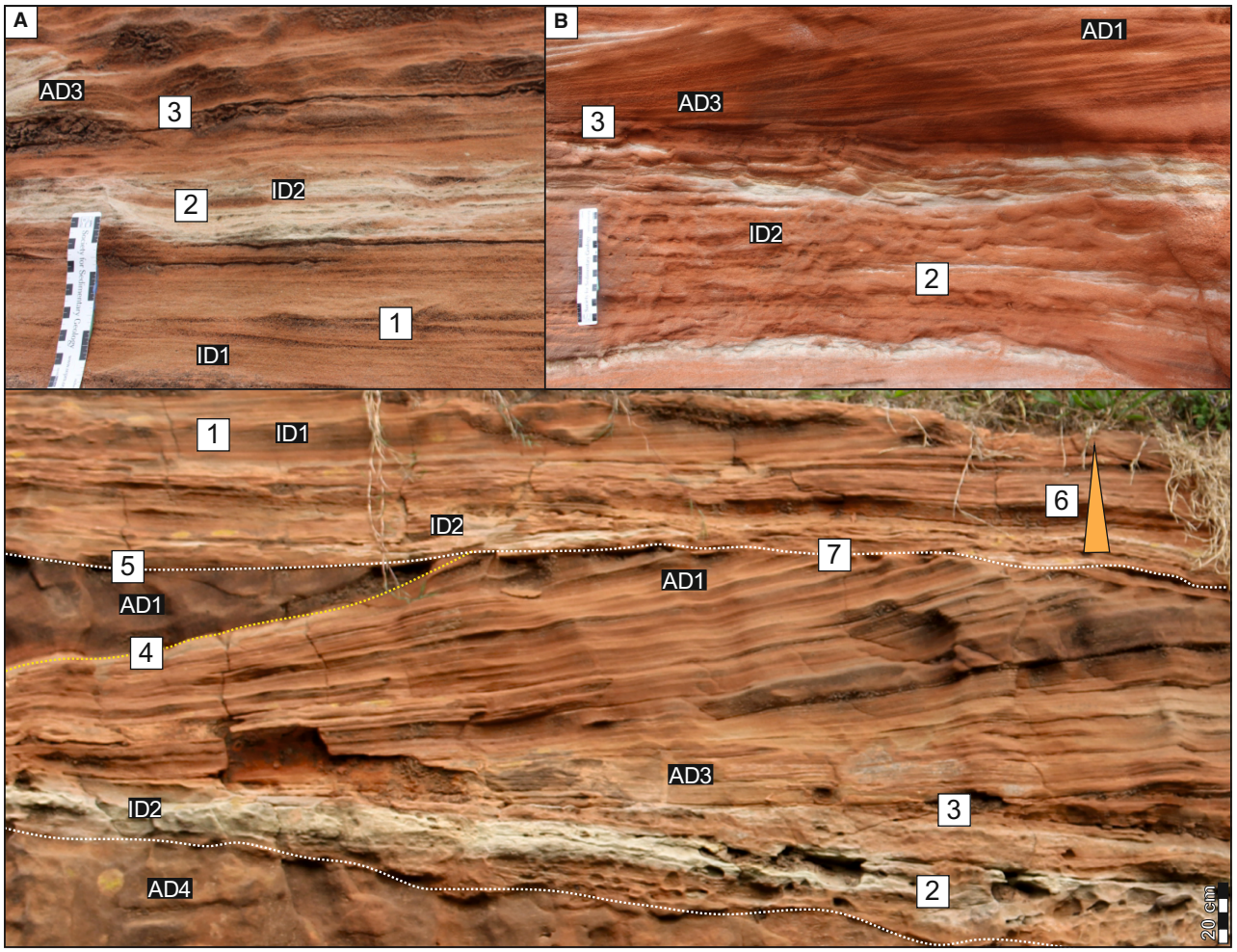

Fig. 16. Examples of climbing and non-climbing accumulation in the Sherwood Sandstone Group. (A) and (B) Climbing accumulation: aeolian dune sets (Aeolian Dune Facies (AD) 1 – Aeolian Dune Facies (AD) 4) overlie damp interdunes (Interdune Facies (ID) 2); the toesets of the interdune interfinger with interdune deposits suggesting that interdune deposition was synchronous with dune migration and accumulation. (C) Non-climbing accumulation: aeolian dune sets are sharply truncated by overlying interdune. Numbers denote points of interest described below. '1' Wind-ripple strata; '2' wavy lamination; '3' interfingering of dune toesets and underlying damp interdune; '4' reactivation surface; '5' scour surface; '6' drying upward trend (transition from wet/damp to dry interdune); '7' sharp truncation of aeolian dune.

found in DASA (Fig. 13; Table 3); the factors that influence angle of climb in aeolian systems are discussed below in these contexts.

Rate of accommodation generation

The subsidence histories of rift basins can affect the angle of climb – and consequently the accumulation of wet-interdune strata – by influencing rates of accommodation generation. In active rift basins, subsidence tends to occur in a punctuated (episodic) manner, in response to discrete events or phases be associated with faulting, whereby accommodation is generated rapidly (Leeder & Gawthorpe, 1987; Newell, 2000). These phases are likely associated with rapid rises in the level of the accumulation surface; dunes and interdunes may accumulate via bedform climbing to fill the available accommodation (Crabaugh & Kocurek, 1993; Kocurek & Havholm, 1993; Carr-Crabaugh & Kocurek, 1998).

However, under conditions of unsteady accommodation generation, aeolian accumulation may be punctuated by episodes of sediment bypass or erosion, when accumulation

Table 3. Comparison of Sherwood Sandstone Group (SSG) architectural elements with Database of Aeolian Sedimentary Architecture (DASA) outputs.

	Mean	Median	SD	N	*P*-value (comparison with SSG)
Dune Thickness (m)					
SSG	0.92	0.75	0.70	59	–
All Systems in DASA	5.19	2.00	8.34	1992	**<0.01**
Greenhouse Systems	6.13	2.50	9.48	1344	**<0.01**
Rift Basin Systems	2.30	1.25	3.23	457	**<0.01**
Wet Systems	2.81	1.50	6.13	996	**0.02**
Marginal Systems	2.24	1.40	6.31	670	0.11
Mesozoic Systems	7.72	4.00	9.80	871	**<0.01**
Dry Interdune Thickness (m)					
SSG	0.30	0.18	0.23	14	–
All Systems in DASA	1.59	0.50	2.24	85	**0.03**
Greenhouse Systems	2.21	1.25	2.26	37	**<0.01**
Rift Basin Systems	1.12	0.50	1.96	26	0.13
Wet Systems	1.10	0.33	2.12	48	0.18
Marginal Systems	0.85	0.20	2.10	49	0.33
Mesozoic Systems	2.06	1.25	1.98	31	**<0.01**
Wet Interdune Thickness (m)					
SSG	0.29	0.25	0.19	29	–
All Systems in DASA	1.27	0.30	2.56	170	**0.04**
Greenhouse Systems	1.63	0.40	3.10	102	**0.02**
Rift Basin Systems	1.27	0.50	2.60	58	0.05
Wet Systems	1.17	0.25	2.48	152	0.06
Marginal Systems	0.41	0.25	0.46	77	0.20
Mesozoic Systems	4.91	5.00	4.21	19	**<0.01**

Note: *P*-values highlighted in bold are statistically significant.

generation stalls or ceases at times when accommodation is generated only very slowly, for example due to sediment compaction (Cosgrove *et al.*, 2023a,b). This would enable only slow accumulation of wet-interdune strata via a non-climbing mechanism, with the angle of climb fluctuating close to zero. Preservation of dunes under this circumstance occurs in response to punctuated episodes of water-table rise and the slow generation of accommodation. Hence, sediment bypass is dominant, resulting in a stratigraphic record that represents a series of amalgamated wet-interdune elements that may be separated from time to time by the fortuitous accumulation of thin sets of aeolian dune strata when accommodation and climate allow (Simpson & Loope, 1985). This style of preserved stratigraphic architecture records the migration of isolated aeolian dunes across wet interdune flats where the angle of climb was essentially zero for prolonged periods. Thus, preserved successions may contain numerous bypass supersurfaces (cf. Crabaugh & Kocurek, 1993). However, such surfaces are difficult to identify since they are effectively diastems (paraconformities) that separate packages of similar strata that become vertically stacked, potentially over time periods of tens to hundreds of thousands of years (Heckel, 1980; Loope, 1988; Crabaugh & Kocurek, 1993).

Given the rifting history of the Cheshire Basin, alternating episodes of climbing (immediately following an episode of fault activity) and non-climbing (during periods of tectonic quiescence) accumulation of aeolian dune and wet-interdune strata was likely. The basin evolved via fault-controlled subsidence from the early Permian and Triassic and it experienced multiple phases of subsidence and uplift throughout the Mesozoic (Evans *et al.*, 1993). This subsidence history could have potentially caused the angles of climb to fluctuate between positive and slightly negative values. Consequently, this may have, led to the formation of amalgamated wet-interdune elements at times (Kocurek & Havholm, 1993). The preservation of thinner and shorter dune-set elements between amalgamated interdune deposits suggests, albeit speculatively, that they may have originated from small, isolated dune forms ('lensoidal accumulations',

sensu McKee & Moiola, 1975; Simpson & Loope, 1985; Loope & Simpson, 1992; Kocurek & Havholm, 1993; Fig. 14).

Rate of sediment supply

Changes in dune size may be associated with variations in sediment supply over both time and space. The rate of sediment supply to the Cheshire Basin during the Triassic varied in a complex way, and was likely influenced by a variety of factors, including tectonics, sea-level and climate changes. The tectonic history of the basin – discussed above – may have influenced the rate of sediment supply. The basin underwent multiple episodes of subsidence and uplift, which may have affected the connectivity to sediment sources and the drainage patterns within the region. Episodes of fault-generated, rapid tectonic subsidence may have resulted in the temporary disconnection of the Cheshire Basin from the adjoining Stafford and Shropshire basins to the south (cf. Newell, 2018). This may have at least temporarily curtailed the evolution of through-going fluvial systems and may have allowed the Cheshire Basin to act as a sediment trap for detritus sourced from nearby uplands by local rivers (Burgess *et al.*, 2024) and aeolian processes. Moreover, it may have promoted the construction and accumulation of aeolian sedimentary systems at a time when the potential for fluvial reworking of aeolian sediments by major through-going rivers was reduced.

In the Cheshire Basin, pebble-bearing fluvial deposits with broadly northward-directed palaeocurrents occur at multiple stratigraphic levels within the Sherwood Sandstone Group (Thompson, 1970a,b). Associated provenance indicators, suggest the episodic re-emergence of a major through-going river system, which transported sediment from sources in the Armorican Massif northward (Tyrrell *et al.*, 2012; Newell, 2018). During episodic hiatuses in subsidence, or during phases dominated by slow thermal subsidence, the Cheshire Basin may have been reconnected with basins to the south, allowing the re-establishment of the major through-going river systems. This, in turn, could have inhibited the development of major aeolian dune fields.

Climatic conditions, particularly changes in aridity and precipitation patterns, could also have affected sediment supply to the Cheshire Basin, therefore influencing dune sizes and the regional angle of bedform climb. Climate changes and their effects on the level of the water table are discussed below.

Water table rise and fall

In the Sherwood Sandstone Group, both dry (ID1) and damp (ID2) interdune deposits are documented; vertical and lateral transitions from wet or damp interdunes to dry interdunes are observed in outcrop (Figs 5 and 9 to 11). This indicates changes in the level of the water table with respect to the depositional surface over space and/or time. In dry interdunes, the water table lies below the level of the depositional surface during sediment accumulation. In wet or damp interdunes, the water table or its capillary fringe are in contact with the depositional surface during sediment accumulation. Such changes in the position of the water table can be relative or absolute. Absolute changes can occur, for example, owing to a shift to a more humid climate. Yet, a relative rise of the water table can take place even if the absolute level remains static, in cases where an aeolian accumulation subsides beneath a static water table (Kocurek & Havholm, 1993). Rises and falls in the water table (whether absolute or relative) affect the availability of sediment for dune construction and cause dunes to expand at the expense of interdunes, and vice versa.

Calcretes (caliche) within the Sherwood Sandstone Group (e.g. Schmid *et al.*, 2006) and extensive evaporites within the MMG (e.g. Porter & Gallois, 2008), indicate arid or semi-arid and well-drained conditions, where water loss through evaporation exceeded water input through precipitation. The fluvial deposits associated closely with the aeolian deposits of the Sherwood Sandstone Group suggest that there must have been considerable precipitation at the basin margin else elsewhere in the upstream catchment area, to enable temporary streamflow through arid terrains (Newell, 2018). This has been attributed to intense monsoonal precipitation and is supported by orientations of cross-beds in aeolian dunes that indicate that the Cheshire Basin was situated within a north-easterly trade-wind belt (Glennie, 1997). The orientation of the cross-beds is compatible with a location within the trade-wind belt, which is supported by palaeolatitudinal constraints and is consistent with the Cheshire Basin being located within the continental interior of Pangea (Newell, 2018).

The time period over which the Sherwood Sandstone Group was deposited, is also

associated with high-amplitude perturbations in carbon isotope curves, coinciding with the end-Permian mass extinction event and extending into the Early Triassic (refer to Payne & Kump, 2007; Radley & Coram, 2015; Newell, 2018). These isotopic excursions, which suggest an increase in the proportion of heavier carbon isotopes in the atmosphere, are correlated with the major volcanic eruptions of the Siberian Traps (Burgess & Bowring, 2015). These periods also align with times of low biological diversity in both terrestrial and marine realms, with a hiatus in coal deposition and with the absence of coral reefs (Chen & Benton, 2012; Benton & Newell, 2014).

The isotopic excursions observed in the Early Triassic are speculatively linked to climatic perturbations, influencing the wet and dry aeolian deposits of the Sherwood Sandstone Group. Although the exact relationship between positive CIEs (carbon isotope excursions) and climatic conditions is not universally agreed upon, there is an intriguing possibility that these warmer episodes associated with volcanic carbon influx may have influenced fluctuations between drier and wetter conditions. Thus, increased global temperatures during the early Triassic due to the greenhouse effect caused by volcanic activity might have enhanced regional hydrological cycles, increasing rainfall and changing conditions from dominantly arid to dominantly humid (cf. Jewuła *et al.*, 2021).

These climatic oscillations and the associated regional hydrological responses would have left distinct signatures in the sedimentary record. The expansion and contraction of interdune units within the Sherwood Sandstone Group could reflect the dynamic shifts between arid and more humid conditions over time. Interdunes of the Sherwood Sandstone Group may have expanded and contracted over time as conditions at the accumulation surface may have varied cyclically from relatively drier to damp and relatively wetter, in response to variation in the level of the water table. Additionally, direct inputs of surface water through precipitation may also account for damp to wet variations in the interdune palaeoenvironments.

Controlling factors

Statistical analysis suggests that the sedimentary architecture of the aeolian deposits of the Sherwood Sandstone Group are influenced by: (i) their deposition in a rift basin setting (Griffiths *et al.*, 2003; Ziegler & Dèzes, 2006); (ii) their physiographic location in a dune-field margin (Thompson, 1970a,b; Mountney & Thompson, 2002); and (iii) their deposition in a wet aeolian system (Thompson, 1970a,b; Mountney & Thompson, 2002). The aeolian architectural elements of the Sherwood Sandstone Group (dune sets and damp and wet-interdune deposits) differ significantly in thickness statistics from: (i) other greenhouse deposits; (ii) other Mesozoic deposits (Table 3; Fig. 13). In all instances, the architectural elements of the Sherwood Sandstone Group are significantly thinner, on average, than those seen in these other groups of successions (Table 3; Fig. 13). Given that the aeolian deposits of the Sherwood Sandstone Group have been compared with 87 case studies, which: (i) have a global distribution; (ii) cover a variety of palaeoenvironmental settings; and (iii) range from Precambrian to Cenozoic in age, significant differences in architectural-element thickness are unsurprising.

However, there remains a question as to why Sherwood Sandstone Group aeolian architectural elements are on average thinner than those of other comparable greenhouse, Mesozoic aeolian systems (Table 3; Fig. 13). Greenhouse aeolian elements are generally thicker than their icehouse counterparts, perhaps because relatively more humid conditions and higher eustatic sea levels promote elevated water tables that are situated close to, or at, the accumulation surface; this allows aeolian elements to be rapidly sequestered beneath the erosional baseline and thus become protected from post-depositional reworking (Kocurek *et al.*, 2001; Cosgrove *et al.*, 2021b, 2022). In greenhouse climates, dunes are often stabilized by vegetation that thrives under relatively more humid conditions (Cosgrove *et al.*, 2021b, 2022); the attenuated diversity and abundance of vegetation in the Cheshire Basin following the Permian–Triassic mass extinction may partly explain the reduced average thickness of Sherwood Sandstone Group dune sets compared to other greenhouse aeolian deposits.

The major controls on aeolian system behaviour and resultant preserved aeolian architecture of the Sherwood Sandstone Group are illustrated through a series of conceptual graphs outlined in Fig. 17.

Figure 17A shows basin subsidence in the Cheshire Basin, driven by fault-generated rifting, which leads to episodic rapid accommodation creation, interrupted by periods of stagnant accommodation. Fig. 17B depicts how sediment

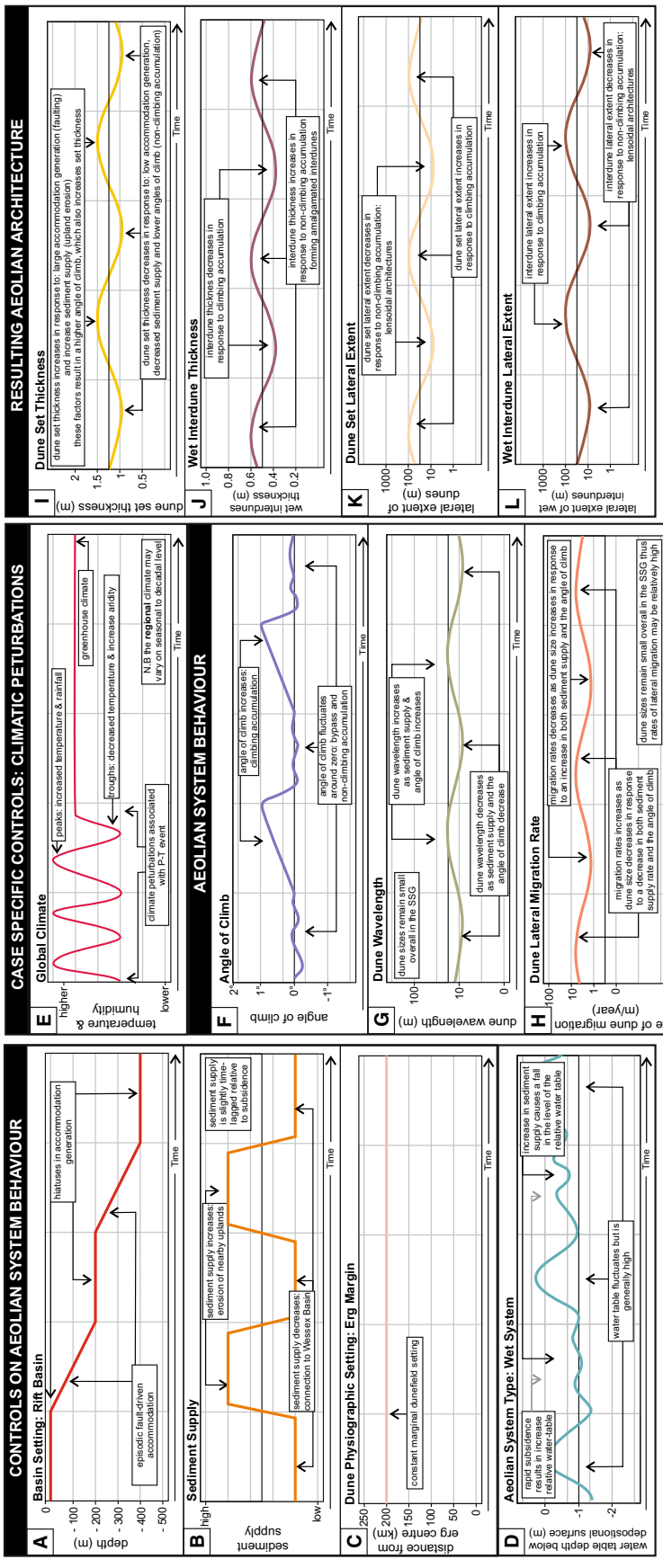

Fig. 17. Conceptual graphs describing the major controls on aeolian system behaviour and the resulting aeolian architecture of the Sherwood Sandstone Group. (A) Basin subsidence; (B) sediment supply rates to the Cheshire Basin; (C) dune-field physiographic setting; (D) aeolian system type; (E) carbon isotope curves; (F) angle of climb in response to the rate of accommodation generation; (G) dune wavelength; (H) rate of lateral migration; (I) dune set thickness; (J) wet interdune thickness; (K) and (L) lateral continuity of dunes and interdunes. NB. All scales are indicative.

supply rates to the Cheshire Basin were influenced by faulting episodes that temporarily disconnected it from the upstream basins, potentially allowing the Cheshire Basin to act as a sediment trap for sediment locally supplied from surrounding uplands (Newell, 2018). The sediment supply rate encompasses the total amount of sediment delivered to the basin; however, some of this sediment may bypass the aeolian system. Fig. 17C highlights the location of the study interval in a marginal dune-field physiographic setting (Thompson, 1970a,b; Mountney & Thompson, 2002). Fig. 17D depicts the studied succession as a wet aeolian system with a fluctuating water table, influenced by regional climatic changes (such as monsoonal conditions), but where the relative level of the water table remained high overall due to rapid fault-generated subsidence (Newell, 2018). Fig. 17E presents carbon isotope curves showing significant perturbations coinciding with the End Permian mass extinction and extending into the Triassic period. These isotopic excursions (refer to Payne & Kump, 2007; Radley & Coram, 2015; Newell, 2018), possibly linked to climatic fluctuations, may be indicative of variations in accumulation surface conditions between wetter and drier phases within an overall greenhouse climate context.

The intrinsic behaviour of the aeolian system was influenced by factors A to F. Fig. 17F demonstrates how the angle of climb varied with the rate of accommodation generation: during episodes of fault-generated subsidence, dunes and interdunes likely climbed over one another, whereas during episodes of tectonic quiescence, the angle of climb likely approached zero, leading to non-climbing bypass and only episodic opportunistic accumulation. Fig. 17G shows how changes in dune wavelength likely occurred in response to variations in sediment supply: increased sediment supply resulted in the construction of relatively larger aeolian dunes, though aeolian dunes were likely of modest size in the dune fields of the Cheshire Basin (Mountney & Thompson, 2002). Fig. 17H illustrates how the rate of lateral migration was likely inversely related to dune wavelength: smaller aeolian dunes (with small wavelengths) tend to undertake higher rates of lateral migration and thereby accumulate at a lower angle of climb in response to relative water-table rise (the climb angle being determined by the ratio between the rate of bedform migration and the rate of vertical accumulation – Mountney & Thompson, 2002). Factors highlighted in Fig. 17G to I determine the architectural configuration of aeolian elements of the Sherwood Sandstone Group. Fig. 17I explains how dune-set thickness increases with episodes of fault-generated subsidence and associated sediment supply, allowing relatively larger dunes to climb over one another at steeper angles and preserving thicker bed sets. Fig. 17J explains how the preserved thickness of wet interdune elements increases during sustained episodes of zero subsidence: the non-climbing accumulation of numerous successive migrating wet interdunes and the resultant vertical amalgamation of their deposits (Basilici *et al.*, 2021).

CONCLUSIONS

Within the Sherwood Sandstone Group, two main continental depositional environments are identified: (i) a marginal aeolian dune-field system; and (ii) a partly channelized and partly non-channelized fluvial system. Both developed in an arid to semi-arid dryland setting. The aeolian succession represents the preserved deposits of a water-table-influenced aeolian system, whose preservation may have been primarily controlled by changes in the level of the water table. Examples of both climbing and non-climbing dune-interdune behaviours are preserved, as are bypass and deflation supersurfaces.

A quantitative comparison indicates that aeolian deposits of the Sherwood Sandstone Group are statistically similar to other aeolian systems deposited in similar basin settings (rifts), physiographic settings (erg margins) and aeolian system types (wet) (Fig. 13; Table 3). These are inferred as the most important factors governing the thickness of dune and interdune elements.

1 *Basin setting*. Rift basins are characterized by non-linear rates of accommodation generation, associated with episodic fault-induced subsidence. Instantaneous accommodation generation due to normal faulting enables temporary increases in bedform climb. Long episodes of tectonic quiescence with only very slow rates of accommodation generation occur during hiatuses in subsidence; non-climbing aeolian accumulation occurs during these phases. The tectonic basin history may have also affected the connectivity of the Cheshire Basin to adjacent coeval basins, sediment sources and fluvial drainage systems. The basin experienced

repeated episodes of basin subsidence and margin uplift, influencing sediment connectivity and drainage patterns. Fault-induced instantaneous tectonic subsidence possibly temporarily isolated the Cheshire Basin from up-dip basins, potentially turning it into a trap for sediment derived from the denudation of nearby uplands at the basin margin. This encouraged aeolian dune-field construction and accumulation. Conversely, during hiatuses in subsidence or phases of slow thermal subsidence, connections between the Cheshire Basin and the neighbouring Stafford and Needwood basins facilitated the development of major inter-basinal fluvial fairways, hindering significant erg development.

2 *Dune physiographic setting*. In contrast to dune-field centres, marginal areas tend to be characterized by smaller dunes separated by interdune flats. Small dunes (wavelength = *ca* 12–40 m; lateral spacing = *ca* 15–46 m; amplitude = *ca* 5 m) in the Sherwood Sandstone Group are reconstructed from analysis of the proportion of different sedimentary facies (increase in grainflow strata relative to wind-ripple strata). These observations suggest sediment accumulation via small, rapidly migrating transverse or oblique dunes between isolated interdune depressions. Smaller dunes tend to migrate more rapidly than larger dunes, resulting in a lower angle of climb and thinner dune sets for a constant rate of accumulation.

3 *Aeolian system type*. The Sherwood Sandstone Group is the preserved record of a wet aeolian system, in which the water table was episodically in contact with or above the depositional surface. Absolute levels of the water table may have been episodically raised by intense monsoonal precipitation. Rapid fault-related subsidence likely acted to place aeolian interdune and dune toesets beneath this relatively high water table, thereby acting as a mechanism to enable accumulation and preservation.

The results of this study help to constrain the primary controls that govern the accumulation of aeolian systems and the long-term preservation of their deposits. The results are of value for developing aeolian facies models expressing likely associations of aeolian and associated non-aeolian architectural elements, deposited under water-table controlled conditions in dune-field margin settings. Based on the presented data synthesis, quantitative predictions of expected aeolian facies architectures can be made for analogous subsurface aeolian successions.

ACKNOWLEDGEMENTS

We thank AkerBP, Areva (now Orano), BHPBilliton, Cairn India (Vedanta), ConocoPhillips, Chevron, CNOOC, ENI, Equinor, Murphy, Occidental Petroleum, Saudi Aramco, Shell, Tullow, Woodside and YPF for their financial support of the Fluvial, Aeolian & Shallow-Marine Research Group at the University of Leeds. We are grateful to Steven Banham and an anonymous reviewer, to Associate Editor Charlie Bristow, and to Chief Editor Piret Plink-Björklund for their constructive comments and advice.

DATA AVAILABILITY STATEMENT

The data that supports the findings of this study are available in the article and in the Supplementary Material.

REFERENCES

Ahlbrandt, T.S. and **Fryberger, S.G.** (1981) Sedimentary features and significance of interdune deposits. In: *Recent and Ancient Non-Marine Depositional Environments: Models for Exploration* (Eds Ethridge, F.G. and Flore, R.M.), *SEPM. Spec. Publ.*, **31**, 293–314.

Allen, D.J. and **Holloway, S.** (1984) Investigation of the Geothermal Potential of the UK: the Wessex Basin British Geological Survey London.

Al-Masrahy, M.A. and **Mountney, N.P.** (2013) Remote sensing of spatial variability in aeolian dune and interdune morphology in Rub' Al-Khali, Saudi Arabia. *Aeolian Res.*, **11**, 155–170.

Al-Masrahy, M.A. and **Mountney, N.P.** (2015) A classification scheme for fluvial–aeolian system interaction in desert-margin settings. *Aeolian Res.*, **17**, 67–88.

Andrews, S. (1981) Sedimentology of Great Sand Dunes, Colorado. *Soc. Econ. Paleontol. Mineral. Spec. Pub.*, **31**, 279–291.

Armitage, P.J., **Worden, R.H.**, **Faulkner, D.R.**, **Aplin, A.C.**, **Butcher, A.R.** and **Espie, A.A.** (2013) Mercia Mudstone Formation caprock to carbon capture and storage sites: petrology and petrophysical characteristics. *J. Geol. Soc. London.*, **170**, 119–132.

Armitage, P.J., **Worden, R.H.**, **Faulkner, D.R.**, **Butcher, A.R.** and **Espie, A.A.** (2016) Permeability of the Mercia Mudstone: suitability as caprock to carbon capture and storage sites. *Geofluids.*, **16**, 26–42.

Bagnold, R.A. (1941) *The Physics of Blown Sand and Desert Dunes*, p. 265. Methuen & Company, London.

Basilici, G., **Mesquita, A.F.J.**, **Soares, A.V.T.**, **Janočkoc, N.P.**, **Mountney, N.P.** and **Colombera, L.** (2021) A Mesoproterozoic hybrid dry–wet aeolian system: Galho do Miguel Formation, SE Brazil. *Precambrian Res.*, **359**, 106216.

Benton, M.J. and **Newell, A.J.** (2014) Impacts of global warming on Permo–Triassic terrestrial ecosystems. *Gondw. Res.*, **25**, 1308–1337.

Benton, M.J., **Warrington, G.**, **Newell, A.J.** and **Spencer, P.R.** (1994) A review of the British Triassic tetrapod assemblages. In: *In the Shadow of the Dinosaurs* (Eds Fraser, N.C. and Sues, H.D.), pp. 131–160. Cambridge University Press, Cambridge.

Bogle, R., **Redsteer, M.H.** and **Vogel, J.** (2015) Field measurement and analysis of climatic factors affecting dune mobility near Grand Falls on the Navajo Nation, southwestern United States. *Geomorphology*, **228**, 41–51.

Boulghobra, N. (2016) Climatic data and satellite imagery for assessing the aeolian sand deposit and barchan migration, as a major risk sources in the region of In-Salah (Central Algerian Sahara). *Arab J Geosci.*, **9**, 1–15.

Bowman, M.B.J., **McClure, N.M.** and **Wilkinson, D.W.** (1993) *Wytch Farm Oilfield: Deterministic Reservoir Description of the Triassic Sherwood Sandstone*, pp. 1513–1517. Petroleum Geology Conference Series, Geological Society of London, London.

Burgess, S.D. and **Bowring, S.A.** (2015) High-precision geochronology confirms voluminous magmatism before, during, and after Earth's most severe extinction. *Sci. Adv.*, **1**, 1–14.

Burgess, P.M., **Dobromylskyj, E.** and **Lovell-Kennedy, J.** (2024) Probably proximal pebbles? An outcrop-constrained quantitative analysis of clast transport distances in the Lower Triassic Sherwood Sandstone Group, UK. *J. Geol. Soc. London*, **182**. https://doi.org/10.1144/jgs2024-15.

Burley, S.D. (1984) Patterns of diagenesis in the Sherwood sandstone group (Triassic), United Kingdom. *Clay Miner.*, **19**, 403–440.

Campos-Soto, S., **Benito, M.I.**, **Mountney, N.P.**, **Plink-Björklund, P.**, **Quijada, I.E.**, **Suarez-Gonzalez, P.** and **Cobos, A.** (2022) Where humid and arid meet: Sedimentology of coastal siliciclastic successions deposited in apparently contrasting climates. *Sedimentology*, **69**, 975–1027.

Carr-Crabaugh, M. and **Kocurek, G.** (1998) Continental sequence stratigraphy of a wet eolian system: a key to relative sea-level change. In: *Relative Roles of Eustasy, Climate, and Tectonism in Continental Rocks* (Eds Shanley, K. and McCabe, P.), *Soc. Sediment. Res., Spec. Public*, **59**, 213–228.

Carruthers, R.A. (1987) Aeolian sedimentation from the galtymore formation (Devonian), Ireland. In: *Desert Sediments: Ancient and Modern* (Eds Frostick, L.E. and Reid, I.), *Geol. Soc. London Spec. Publ*, **35**, 251–268.

Chadwick, R.A. (1997) Fault analysis of the Cheshire Basin, NW England. In: *Petroleum Geology of the Irish Sea and Adjacent Areas* (Eds Meadows, N.S., Trueblood, S.P., Hardman, M. and Cowan, G.), *Geol. Soc. London, Spec. Public*, **124**, 297–313.

Chadwick, R.A. and **Evans, D.J.** (1995) The timing and direction of Permo-Triassic extension in southern Britain. In: *Permian and Triassic Rifting in Northwest Europe* (Ed. Boldy, S.A.R.), *Geol. Soc. London Spec. Public*, **91**, 161–192.

Chen, Z.Q. and **Benton, M.J.** (2012) The timing and pattern of biotic recovery following the end-Permian mass extinction. *Nat. Geosci.*, **5**(6), 375–383.

Collinson, J.C. (1994) Sedimentary deformational structure. In: *The Geological Deformation of Sediments* (Ed. Maltman, A.), pp. 95–125. Chapman and Hall, London.

Colter, V.S. and **Barr, K.W.** (1975) Recent developments in the geology of the Irish Sea and Cheshire Basins. In: *Petroleum and the Continental Shelf of North West Europe* (Ed. Woodland, A.W.), pp. 61–75. Applied Science Publishers, London.

Cosgrove, G.I.E., **Colombera, L.** and **Mountney, N.P.** (2021a) A database of Eolian Sedimentary Architecture for the characterization of modern and ancient sedimentary systems. *Mar. Pet. Geol.*, **127**, 104983.

Cosgrove, G.I.E., **Colombera, L.** and **Mountney, N.P.** (2021b) Quantitative analysis of the sedimentary architecture of eolian successions developed under icehouse and greenhouse climatic conditions. *Geol. Soc. Am. Bull.*, **133**, 2625–2644.

Cosgrove, G.I.E., **Colombera, L.** and **Mountney, N.P.** (2022) The role of subsidence and accommodation generation in controlling the nature of the aeolian stratigraphic record. *J. Geol. Soc. London*, **179**, jgs2021.

Cosgrove, G.I.E., **Colombera, L.** and **Mountney, N.P.** (2023a) Quantitative analysis of aeolian stratigraphic architectures preserved in different tectonic settings. *Earth Sci. Rev.*, **237**, 104293.

Cosgrove, G.I.E., **Colombera, L.**, **Mountney, N.P.**, **Basilici, G.**, **Mesquita, A.F.** and **Marcus Vinícius Theodoro Soares, M.V.T.** (2023b) Precambrian aeolian systems: a unique record? *Precambrian Res.*, **392**, 107075.

Coward, M.P. (1995) Structural and tectonic setting of the Permo-Triassic basins of northwest Europe. *Geol. Soc. Lond., Spec. Publ.*, **91**, 7–39.

Crabaugh, M. and **Kocurek, G.** (1993) Entrada Sandstone: an example of a wet aeolian system. In: *The Dynamics and Environmental Context of Aeolian Sedimentary Systems* (Ed. Pye, K.), *Geol. Soc. London Spec. Publ*, **72**, 103–126.

Doe, T.W. and **Dott, R.H., Jr.** (1980) Genetic significance of deformed cross bedding – with examples from the Navajo and Weber Sandstones of Utah. *J. Sediment. Res.*, **50**, 793–811.

Downing, R.A., **Allen, D.J.**, **Barker, J.A.**, **Burgess, W.G.**, **Gray, D.A.**, **Price, M.** and **Smith, I.F.** (1984) Geothermal exploration at Southampton in the UK: a case study of a low enthalpy resource. *Energy Explor. Exploit.*, **2**, 327–342.

Evans, C.D.R. (1990) *United Kingdom Offshore Regional Report: The Geology of the Western English Channel and its Western Approaches*. HMSO for the British Geological Survey, London.

Evans, D.J., **Rees, J.G.** and **Holloway, S.** (1993) The Permian to Jurassic stratigraphy and structural evolution of the central Cheshire Basin. *Geol. Soc. Lond.*, **150**, 857–870.

Fryberger, S.G. (1990) Role of water in eolian deposition. In: *Modern and Ancient Eolian Deposits: Petroleum Exploration and Production* (Eds Fryberger, S.G., Krystinik, L.F. and Schenk, C.J.), pp. 1–11. SEPM, Denver.

Fryberger, S.G. and **Schenk, C.J.** (1988) Pin stripe lamination-a distinctive feature of modern and ancient eolian sediments. *Sediment. Geol.*, **55**, 1–15.

García-Hidalgo, J.F., **Temiño, J.** and **Segura, M.** (2002) Holocene eolian sediments on the southern border of the Duero Basin (Spain): origin and development of an eolian system in a temperate zone. *J. Sediment. Res.*, **72**, 30–39.

Glennie, K.W. (1983) Early Permian (Rotliegend) palaeowind of the North Sea. *Sediment. Geol.*, **34**, 120–152.

Glennie, K.W. (1990) Lower Permian – Rotliegend. In: *Introduction to the Petroleum Geology of the North Sea* (Ed. Glennie, K.W.), pp. 120–152. Blackwell Science, Oxford.

Glennie, K.W. (1997) Recent advances in understanding the Southern North Sea Basin: a summary. *Geol. Soc. Lond. Spec. Publ.*, **123**, 17–29.

Granja, H.M., **De Groot, T.A.M.** and **Costa, A.L.** (2008) Evidence for Pleistocene wet aeolian dune and interdune accumulation, S. Pedro da Maceda, north-west Portugal. *Sedimentology*, **55**, 1203–1226.

Griffiths, K.J., **Shand, P.** and **Ingram, I.** (2003) Baseline report series: 8. The Permo-Triassic sandstones of Manchester and east Cheshire. British Geological Survey Commissioned Report CR/03/265N.

Groh, C., **Wierschem, A.**, **Aksel, N.**, **Rehberg, I.** and **Kruelle, C.A.** (2008) Barchan dunes in two dimensions: experimental tests for minimal models. *Phys. Rev. E.*, **78**, 21304.

Gross, E.C., **Carr, M.** and **Jobe, Z.R.** (2023) Three-dimensional bounding surface architecture and lateral facies heterogeneity of a wet aeolian system: Entrada Sandstone, Utah. *Sedimentology*, **70**, 145–178.

Hamdan, M.A., **Refaat, A.A.** and **Wahed, M.A.** (2016) Morphologic characteristics and migration rate assessment of barchan dunes in the southeastern Western Desert of Egypt. *Geomorphology*, **257**, 57–74.

Harland, W.B., **Armstrong, R.L.**, **Cox, A.V.**, **Craig, L.E.**, **Smith, A.G.** and **Smith, D.G.** (1990) *A Geologic Time Scale 1989*. Cambridge University Press, Cambridge.

Heckel, P.H. (1980) Paleogeography of Eustatic Model for Deposition of Midcontinent Upper Pennsylvanian Cyclothems. In: *Paleozoic Paleogeography of the West-Central United States* (Eds Fouch, T.D. and Magathan, E.R.), *SEPM Rocky Mountain Sec., Rocky Mountain Paleogeogr. Symp.*, **1**, 197–215.

Hême de Lacotte, V.J.P. and **Mountney, N.P.** (2022) A classification scheme for sedimentary architectures arising from aeolian-fluvial system interactions: permian examples from southeast Utah, USA. *Aeolian Res.*, **58**, 100815.

Herries, R.D. (1993) Contrasting styles of Fluvio-Aeolian interaction at a downwind Erg Margin: Jurassic Kayenta-Navajo Transition, Northern Arizona, USA. In: *Characterization of Fluvial and Aeolian Reservoirs* (Eds North, C.P. and Prosser, D.J.), *Geol. Soc. London Spec. Publ.*, **73**, 199–218.

Herries, R.D. and **Cowan, G.** (1997) Challenging the sheetflood myth: the role of water-table-controlled sabkha deposits in redefining the depositional model for the Ormskirk Sandstone Formation (Lower Triassic), East Irish Sea Basin. In: *Petroleum Geology of the Irish Sea and Adjacent Areas* (Eds Meadows, N.S., Trueblood, S.P., Hardman, M. and Cowan, G.), *Geol. Soc. London Spec. Publ.*, **124**, 253–276.

Hersen, P., **Douady, S.** and **Andreotti, B.** (2002) Relevant length scale of barchan dunes. *Phys. Rev. Lett.*, **89**, 264–301.

Hirst, C.M., **Gluyas, J.G.**, **Adams, C.A.**, **Mathias, S.A.**, **Bains, S.** and **Styles, P.** (2015) UK low enthalpy geothermal resources: the Cheshire Basin. Proceedings World Geothermal Congress, Melbourne, Australia.

Hogg, A.J.C., **Mitchell, A.W.** and **Young, S.** (1996) Predicting well productivity from grain size analysis and logging while drilling. *Petrol. Geosci.*, **2**, 1–15.

Holloway, S., **Milodowski, A.E.**, **Strong, G.E.** and **Warrington, W.** (1989) The Sherwood sandstone group (Triassic) of the Wessex Basin, southern England. *Proc. Geol. Assoc.*, **100**, 383–394.

Horowitz, D.H. (1982) Geometry and origin of large-scale deformation structures in some ancient wind-blown sand deposits. *Sedimentology*, **29**, 155–180.

Hotta, S., **Kubota, S.**, **Katori, S.** and **Horikawa, K.** (1984) Sand transport by wind on sand surface. *Coast. Eng.*, **2**, 1265–1281.

Hounslow, M.W. and **McIntosh, G.** (2003) Magnetostratigraphy of the Sherwood Sandstone Group (Lower and Middle Triassic), south Devon, UK: detailed correlation of the marine and nonmarine Anisian. *Palaeogeogr. Palaeoclimatol. Palaeoecol.*, **193**, 325–348.

Hummel, G. and **Kocurek, G.** (1984) Interdune areas of the Back-Island dune field, North Padre-Island, Texas. *Sediment. Geol.*, **39**, 1–26.

Hunter, R.E. (1977a) Terminology of cross-stratified sedimentary layers and climbing ripple structures. *J. Sediment. Petrol.*, **47**, 697–706.

Hunter, R.E. (1977b) Basic types of stratification in small eolian dunes. *Sedimentology*, **24**, 361–387.

Hunter, R.E. (1981) Stratification Styles in Eolian Sandstones: some Pennsylvanian to Jurassic Examples from the Western Interior USA. In: *Recent and Ancient Non-Marine Depositional Environments: Models for Exploration* (Eds Ethridge, F.G. and Flore, R.M.), *SEPM Spec. Publ.*, **31**, 315–329.

Jewuła, K., **Trela, W.** and **Fijałkowska-Mader, A.** (2021) Sedimentary and pedogenic record of seasonal humidity during the Permian-Triassic transition on the SE margin of Central European Basin (Holy Cross Mountains, Poland). *Palaeogeogr. Palaeoclimatol. Palaeoecol.*, **564**, 110154.

Jones, L.S. and **Blakey, R.C.** (1997) Eolian-fluvial interaction in the Page Sandstone (Middle Jurassic) in south-central Utah, USA—a case study of erg-margin processes. *Sediment. Geol.*, **109**, 181–198.

Jones, B. and **Ng, K.C.** (1988) The structure and diagenesis of rhizoliths from Cayman Brac, British West Indies. *J. Sediment. Petrol.*, **58**, 457–467.

Kocurek, G. (1981a) Significance of interdune deposits and bounding surfaces in aeolian dune sands. *Sedimentology*, **28**, 753–780.

Kocurek, G. (1999) The aeolian rock record. In: *Aeolian Environments Sediments and Landforms* (Eds Goudie, A.S., Livingstone, I. and Stokes, S.), pp. 239–259. John Wiley and Sons Ltd, Chichester.

Kocurek, G. (1981b) Erg reconstruction – the Entrada Sandstone (Jurassic) of northern Utah and Colorado. *Palaeogeogr. Palaeoclimatol. Palaeoecol.*, **36**, 125–153.

Kocurek, G. and **Fielder, G.** (1982) Adhesion structures. *J. Sediment. Petrol.*, **52**, 1229–1241.

Kocurek, G. and **Havholm, K.G.** (1993) Eolian sequence stratigraphy – a conceptual framework. In: *Siciliclastic Sequence Stratigraphy* (Eds Weimer, P. and Posamentier, H.W.), *AAPG Mem.*, **58**, 393–409.

Kocurek, G. and **Lancaster, N.** (1999) Aeolian system sediment state: theory and Mojave Desert Kelso dune field example. *Sedimentology*, **46**(3), 505–515.

Kocurek, G., **Robinson, N.I.** and **Sharp, J.M., Jr.** (2001) The response of the water table in coastal aeolian systems to changes in sea level. *Sediment. Geol.*, **139**(1), 1–13.

Kocurek, G., **Townsley, M.**, **Yeh, E.**, **Havholm, K.** and **Sweet, M.L.** (1992) Dune and dune-field development on Padre-Island, Texas, with implications for interdune deposition and water-table-controlled accumulation. *J. Sediment. Petrol.*, **62**, 622–635.

Lancaster, N. (1992) Relations between dune generations in the Gran Desierto, Mexico. *Sedimentology*, **39**, 631–644.

Lancaster, N. (1995) Response of eolian geomorphic systems to minor climate change: examples from the southern Californian deserts. *Geomorphology*, **19**, 333–347.

Lancaster, N. and **Teller, J.T.** (1988) Interdune deposits of Namib Sand Sea. *Sediment. Geol.*, **55**, 91–107.

Langford, R.P. (1989) Fluvial–aeolian interactions: part 1, modern systems. *Sedimentology*, **36**, 1023–1035.

Langford, R.P. and **Chan, M.A.** (1988) Flood surfaces and deflation surfaces within the Cutler Formation and Cedar Mesa Sandstone (Permian), southeastern Utah. *Geol. Soc. Am. Bull.*, **100**, 1541–1549.

Leeder, M.R. and **Gawthorpe, R.L.** (1987) *Sedimentary Models for Extensional Tilt-Block/Half-Graben Basins*, pp. 139–152. Geological Society, London.

Loope, D.B. (1988) Rhizoliths and ancient aeolianites. *Sed. Geol.*, **56**, 301–314.

Loope, D.B. and **Simpson, E.L.** (1992) Significance of thin sets of eolian crossstrata. *J. Sediment. Res.*, **62**, 849–859.

Loope, D.B., **Swinehart, J.B.** and **Mason, J.P.** (1995) Dune-dammed paleovalleys of the Nebraska Sand Hills-intrinsic versus climatic controls on the accumulation of lake and marsh sediments. *Geol. Soc. Am. Bull.*, **107**, 396–406.

Loope, D.B., **Elder, J.F.** and **Sweeney, M.R.** (2012) Downslope coarsening in aeolian grainflows of the Navajo Sandstone. *Sed. Geol.*, **265**, 156–162.

Lopez, M. and **Mader, D.** (1985) Gravelly and Sandy Braidplain Evolving into Floodplain and Playa Lake Deposits and Vice Versa in the Buntsandstein-Facies Sediments and Marine Incursions in the Triassic of the Lodève Region (Southern France) Short Communication. In: *Aspects of Fluvial Sedimentation in the Lower Triassic Buntsandstein of Europe*, pp. 509–518. Springer, Berlin Heidelberg.

Maidwell, F.T. (1911) Notes on footprints from the Keuper of Runcorn Hill. *Proc. Liverpool Geol. Soc.*, **11**, 140–152.

Maidwell, F.T. (1914) Some sections in the Lower Keuper of Runcorn Hill. *Proc. Liverpool Geol. Soc.*, **12**, 40–52.

Maidwell, F.T. (1915) Some sections in the Lower Keuper of Runcorn Hill – II. *Proc. Liverpool Geol. Soc.*, **12**, 14141–14149.

McKee, E.D. and **Moiola, R.J.** (1975) Geometry and growth of the White Sands dunes field, New Mexico. *J. Res. U. S. Geol. Surv.*, **3**, 59–66.

Mckee, E.D., **Douglass, J.R.** and **Rittenhouse, S.** (1971) Deformation of lee side laminae in eolian dunes. *Geol. Soc. Am. Bull.*, **82**, 359–378.

McKenna-Neuman, C. and **Nickling, W.G.** (1989) A theoretical and wind tunnel investigation of the effect of capillarity water on the entrainment of sediment by wind. *Can. J. Soil Sci.*, **69**, 79–96.

McKie, T., **Aggett, J.** and **Hogg, A.J.C.** (1998) Reservoir architecture of the upper Sherwood sandstone, Wytch Farm field, southern England. *Geol. Soc. Spec. Pub.*, **133**, 399–406.

Meadows, N.S. (2006) The correlation and sequence architecture of the Ormskirk sandstone formation in the Triassic Sherwood sandstone group of the East Irish Sea Basin, NW England. *Geol. J.*, **41**, 93–122.

Meadows, N.S. and **Beach, A.** (1993) *Controls on reservoir quality in the Triassic Sherwood sandstone of the Irish sea*, pp. 823–833. Petroleum Geology Conference Series, Geological Society of London, London.

Miall, A.D. (1977) A review of the braided river depositional environment. *Earth Sci. Rev.*, **13**, 1–62.

Miall, A.D. (1978) Lithofacies types and vertical profile models in braided river deposits: a summary. In: *Fluvial Sedimentology* (Ed. Miall, A.D.), *Can. Soc. Petrol. Geol. Mem.*, **5**, 597–604.

Miall, A.D. (1988) Reservoir heterogeneities in fluvial sandstones: lessons from outcrop studies. *Am. Assoc. Petrol. Geol. Bull.*, **72**, 682–697.

Mount, J.F. and **Cohen, A.S.** (1984) Petrology and geochemistry of rhizoliths from Plio-Pleistocene fluvial and marginal lacustrine deposits, east Lake Turkana, Kenya. *J. Sediment. Res.*, **54**(1), 263–275.

Mountney, N.P. (2006) Periodic accumulation and destruction of aeolian erg sequences in the Permian Cedar Mesa Sandstone, White Canyon, southern Utah, USA. *Sedimentology*, **53**, 789–823.

Mountney, N.P. (2012) A stratigraphic model to account for complexity in aeolian dune and interdune successions. *Sedimentology*, **59**, 964–989.

Mountney, N.P. and **Howell, J.** (2000) Aeolian architecture, bedform climbing and preservation space in the Cretaceous Etjo Formation, NW Namibia. *Sedimentology*, **47**, 825–849.

Mountney, N.P. and **Jagger, A.** (2004) Stratigraphic evolution of an aeolian erg margin system: the Permian Cedar Mesa Sandstone, SE Utah, USA. *Sedimentology*, **51**, 713–743.

Mountney, N.P. and **Russell, A.J.** (2009) Aeolian dune field development in a water table-controlled system: Skeiðarársandur, southern Iceland. *Sedimentology*, **56**, 2107–2131.

Mountney, N.P. and **Thompson, D.B.** (2002) Stratigraphic evolution and preservation of aeolian dune and damp/wet interdune strata: an example from the Triassic Helsby Sandstone Formation, Cheshire Basin, UK. *Sedimentology*, **49**, 805–834.

Newell, A.J. (2000) Fault activity and sedimentation in a marine rift basin (Upper Jurassic, Wessex Basin, UK). *J. Geol. Soc. London*, **157**, 83–92.

Newell, A.J. (2006) Calcrete as a source of heterogeneity in Triassic fluvial sandstone aquifers (Otter Sandstone Formation, SW England). *Geol. Soc. Lond., Spec. Publ.*, **263**(1), 119–127.

Newell, A.J. (2018) Rifts, rivers and climate recovery: a new model for the Triassic of England. *Proc. Geol. Assoc.*, **129**, 352–371.

Newell, D.L., **Kaszuba, J.P.**, **Viswanathan, H.S.**, **Pawar, R.J.** and **Carpenter, T.** (2008) Significance of carbonate buffers in natural waters reacting with supercritical CO_2: implications for monitoring, measuring and verification (MMV) of geologic carbon sequestration. *Geophys. Res. Lett.*, **35**, 2008GL035615.

Nickling, W.G., **McKenna Neuman, C.** and **Lancaster, N.** (2002) Grainfall processes in the lee of transverse dunes, Silver Peak, Nevada. *Sedimentology*, **49**, 191–209.

Nield, J.M., **Wiggs, G.F.S.**, **Baddock, M.C.** and **Hipondoka, M.H.T.** (2017) Coupling leeside grainfall to avalanche characteristics in aeolian dune dynamics. *Geology*, **45**, 271–274.

Øxnevad, I.E.I. (1991) *Aeolian and Mixed Aeolian-Subaqueous Sedimentation in Modern and Ancient Sub-Tropical Desert Basins: Examples from the Sahara and Permo-Triassic of NW Europe*. Unpubl. DSc Thesis, p. 161. University of Bergen, Bergen.

Payne, J.L. and **Kump, L.R.** (2007) Evidence for recurrent Early Triassic massive volcanism from quantitative

interpretation of carbon isotope fluctuations. *Earth Planet. Sci. Lett.*, **256**, 264–277.

Payton, R.L., **Fellgett, M.**, **Clark, B.L.**, **Chiarella, D.**, **Kingdon, A.** and **Hier-Majumder, S.** (2021) Pore-scale assessment of subsurface carbon storage potential: implications for the UK Geoenergy Observatories project. *Pet. Geosci.*, **27**, 92.

Picard, D.M. and **High, L.R.** (1973) Stratification. In: *Developments in Sedimentology* (Eds Picard, D.M. and High, L.R.), Vol. **17**, pp. 143–188. Elsevier, London.

Plant, J.A., **Jones, D.G.** and **Haslam, H.W.** (1999) *The Cheshire Basin: Basin Evolution, Fluid Movement and Mineral Resources in a Permo-Triassic Rift Setting*. British Geological Survey, Nottingham.

Porter, R.J. and **Gallois, R.W.** (2008) Identifying fluvio–lacustrine intervals in thick playa-lake successions: an integrated sedimentology and ichnology of arenaceous members in the mid–late Triassic Mercia Mudstone Group of south-west England, UK. *Palaeogeogr. Palaeoclimatol. Palaeoecol.*, **270**, 381–398.

Pulvertaft, T.C.R. (1985) Aeolian dune and wet interdune sedimentation in the Middle Proterozoic Dala-Sandstone, Sweden. *Sed. Geol.*, **44**, 93–111.

Purvis, K. and **Wright, V.P.** (1991) Calcretes related to phreatophytic vegetation from the Middle Triassic Otter Sandstone of south-west England. *Sedimentology*, **38**, 539–551.

Radley, J.D. and **Coram, R.A.** (2015) Derived Skolithos pipe rock in the Budleigh Salterton Pebble Beds (Early Triassic, East Devon, UK). *Proc. Geol. Assoc.*, **126**, 220–225.

Reading, H.G. (Ed) (1986) *Sedimentary Environments and Facies*, 2nd edn. Blackwell Scientific, Boston, MA.

Rodríguez-López, J.P., **Clemmensen, L.B.**, **Lancaster, N.**, **Mountney, N.P.** and **Veiga, G.D.** (2014) Archean to Recent aeolian sand systems and their sedimentary record: current understanding and future prospects. *Sedimentology*, **61**, 1487–1534.

Romain, H.G. and **Mountney, N.P.** (2014) Reconstruction of 3D eolian-dune architecture from 1D core data through adoption of analogue data from outcrop. *AAPG Bull.*, **98**, 1–22.

Rubin, D.M. (1987) Cross-bedding, bedforms and palaeocurrents. *SEPM Conc. Sedimentol. Paleontol.*, **1**, 187.

Rubin, D.M. and **Hunter, R.E.** (1983) Reconstructing bedform assemblages from compound crossbedding. In: *Eolian Sediments and Processes* (Eds Brookfield, M.E. and Ahlbrandt, T.S.), *Dev. Sedimentol.*, **38**, 407–427.

Ruffell, A. (1995) Evolution and hydrocarbon prospectivity of the Brittany Basin (Western Approaches Trough), offshore north-west France. *Mar. Pet. Geol.*, **12**, 387–407.

Scheidt, S., **Ramsey, M.** and **Lancaster, N.** (2010) Determining soil moisture and sediment availability at White Sands Dune Field, New Mexico, from apparent thermal inertia data. *J. Geophys. Res.*, **112**, F02019.

Schmid, S., **Worden, R.H.** and **Fisher, Q.J.** (2004) Diagenesis and reservoir quality of the Sherwood Sandstone (Triassic), Corrib Field, Slyne Basin, West of Ireland. *Mar. Petrol. Geol.*, **21**, 299–315.

Schmid, S., **Worden, R.H.** and **Fisher, Q.J.** (2006) Sedimentary facies and the context of dolocrete in the Lower Triassic Sherwood Sandstone group: Corrib Field west of Ireland. *Sediment. Geol.*, **187**, 205–227.

Scorgie, J.C., **Worden, R.H.**, **Utley, J.E.P.** and **Roche, I.P.** (2021) Reservoir quality and diagenesis of Triassic sandstones and siltstones from arid fluvial and playa margin environments: a study of one of the UK's earliest producing oilfields. *Mar. Pet. Geol.*, **131**, 105154.

Sherman, D.J. (1990) Evaluation of aeolian sediment sand transport equations using intertidal-zone measurements, Saunton Sands, England. *Sedimentology*, **37**, 385–392.

Simpson, E.L. and **Loope, D.B.** (1985) Amalgamated interdune deposits, White Sands, New Mexico. *J. Sediment. Res.*, **55**, 361–365.

Strahan, A. (1882) *Geology of the Neighbourhood of Chester*, p. 54. Memoir of Geological Survey UK, London.

Taggart, S., **Hampson, G.J.** and **Jackson, M.D.** (2010) High-resolution stratigraphic architecture and lithological heterogeneity within marginal aeolian reservoir analogues. *Sedimentology*, **57**, 1246–1279.

Thompson, D.B. (1969) Dome shaped aeolian dunes in the Frodsham Member of the so-called 'Keuper' Sandstone Formation [Scythian? Anisan: Triassic] at Frodsham, Cheshire (England). *Sediment. Geol.*, **3**, 263–289.

Thompson, D.B. (1970a) The stratigraphy of the so-called Keuper Sandstone Formation (Scythian?-Anisian) in the Permo-Triassic Cheshire Basin. *Q. J. Geol. Soc. Lond.*, **126**, 151–181.

Thompson, D.B. (1970b) Sedimentation of the Triassic (Scythian) red pebbly sandstones in the Cheshire Basin and its margins. *Geol. J.*, **7**, 183–216.

Tooth, S. (2000) Process, form and change in dryland rivers: a review of recent research. *Earth Sci. Rev.*, **51**, 67–107.

Tyrrell, S., **Haughton, P.D.W.**, **Souders, A.K.**, **Daly, J.S.** and **Shannon, P.M.** (2012) Large-scale, linked drainage systems in the NW European Triassic: insights from the Pb isotopic composition of detrital K-feldspar. *J. Geol. Soc. London*, **169**, 279–295.

Walker, R.G. (Ed) (1984) *Facies Models*, 2nd edn. Geoscience Canada Reprint Series, St. Johns, NF.

Warrington, G. and **Ivimey-Cook, H.C.** (1992) Triassic. In: *Atlas of Palaeogeography and Lithofacies* (Eds Cope, J.C.W., Ingham, J.K. and Rawson, P.F.), *Geol. Soc. London, Memoir*, **13**, 97–106.

Warrington, G., **Audley-Charles, M.G.**, **Elliott, R.E.**, **Evans, W.B.**, **Ivemey-Cook, H.C.**, **Kent, P.**, **Robinson, P.L.**, **Shotton, F.W.** and **Taylor, F.M.** (1980) *A Correlation of Triassic Rocks in the British Isles*, Vol. **13**, p. 78. Geological Society of London, London.

Waters, R.A. and **Lawrence, D.J.D.** (1987) Geology of the South Wales Coalfield - Part III: the Country around Cardiff. Memoir of the British Geological Survey, Sheet 263. (England and Wales).

Wilson, I.G. (1973) Ergs. *Sed. Geol.*, **10**, 77–106.

Yaliz, A. and **Chapman, T.** (2003) The Lennox oil and gas field, block 110/15, east Irish sea. *Geol. Soc. Lond. Mem.*, **20**, 87–96.

Yang, X., **Ma, N.**, **Dong, J.**, **Zhu, B.**, **Xu, B.**, **Ma, Z.** and **Liu, J.** (2010) Recharge to the inter-dune lakes and Holocene climatic changes in the Badain Jaran Desert, western China. *Quatern. Res.*, **73**, 10–19.

Yang, J., **Dong, Z.**, **Liu, Z.**, **Shi, W.**, **Chen, G.**, **Shao, T.** and **Zeng, H.** (2019) Migration of barchan dunes in the western Quruq Desert, northwestern China. *Earth Surf. Process. Landf.*, **44**, 2016–2029.

Yang, Z., **Qian, G.**, **Dong, Z.**, **Tian, M.** and **Lu, J.** (2021) Migration of barchan dunes and factors that influence

migration in the Sanlongsha dune field of the northern Kumtagh Sand Sea, China. *Geomorphology*, **378**, 107615.

Ziegler, P.A. and **Dèzes, P.** (2006) Crustal evolution of western and central Europe. *Geol. Soc. London*, **32**, 43–56.

Manuscript received 8 April 2024; revision accepted 4 February 2025

Supporting Information

Additional information may be found in the online version of this article:

Table S1. All DASA data used for statistical analyses.